

Testing Multi-Field Inflation: A Geometric Approach

Courtney M. Peterson¹, Max Tegmark²

¹ *Dept. of Physics, Harvard University, Cambridge, MA 02138, USA*

² *Dept. of Physics & MIT Kavli Institute, Massachusetts Institute of Technology, Cambridge, MA 02139*

(Dated: November 3, 2011)

We develop an approach for testing inflation models with multiple scalar fields by linking geometric and kinematical features of their inflationary Lagrangians to observable quantities like the power spectra, bispectrum, and trispectrum. Our approach also provides geometric intuition for when a complicated multi-field model can be well-approximated by a model with one, two, or a handful of fields. To arrive at these results, we focus on the mode interactions, simplify them using a novel result, and then explore how these interactions depend on the geometry of the inflationary Lagrangian and on the kinematics of the associated field trajectory. In the process, we introduce a multi-field observable β_2 that can potentially distinguish two-field scenarios from scenarios involving three or more effective fields. We also present a multi-field consistency relation, which involves the primordial bispectrum parameter f_{NL} , trispectrum parameter τ_{NL} , and other spectral observables. These combined results provide better intuition into how features in multi-field inflationary Lagrangians translate into cosmic observables.

I. INTRODUCTION

Inflation solves cosmic conundrums such as the horizon, flatness, and relic problems [1–5]. It also offers a mechanism for producing the primordial density fluctuations. According to the inflationary paradigm, our Universe experienced an early period of quasi-exponential expansion. As a result of this inflationary expansion, quantum fluctuations were stretched beyond the causal horizon. Once beyond the horizon, they became locked in as classical perturbations, which eventually initiated the formation of galaxies and large-scale structure [6–11]. Generically, inflation predicts that these classical perturbations should be reflected in a nearly scale-invariant spectrum of primordial density fluctuations at early times.

So far, measurements of the Cosmic Microwave Background (CMB), large-scale structure, supernovae, and gravitational lensing support the inflationary paradigm. These measurements reveal a nearly scale-invariant spectrum of small primordial fluctuations, the presence of superhorizon fluctuations, and that our Universe is essentially flat, as predicted by inflation (see [12] and references therein). But ultimately, we want to use cosmic data not just to test the inflationary paradigm, but to find the particular inflationary model that describes our Universe.

Of the myriad inflationary models, there is good reason to consider models where inflation is driven by multiple scalar fields. Many theories beyond the Standard Model—such as grand unification, supersymmetry, and effective supergravity from string theory—predict the existence of multiple scalar fields, which makes the presence of multiple fields likely during the hot, early Universe. Moreover, multi-field models have become increasingly popular in recent years. These two facts strongly motivate the study of multi-field inflation.

But the sobering reality is that there is a staggeringly large number of multi-field models, making it impractic-

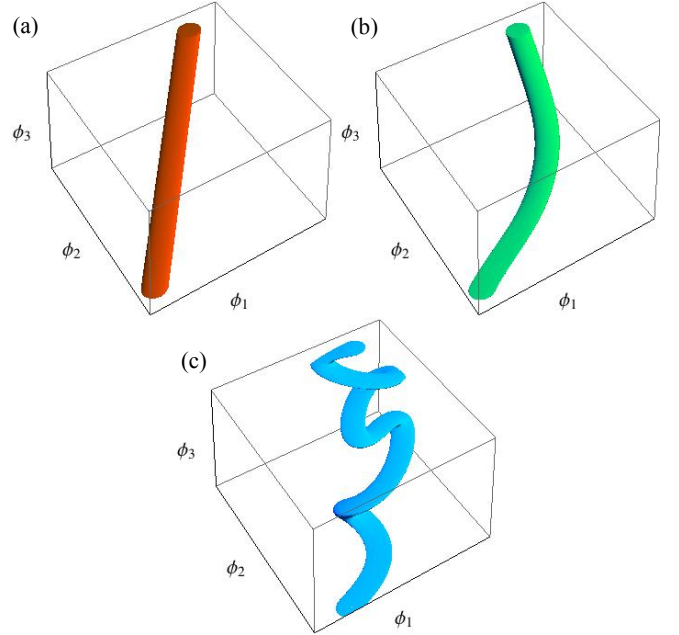


FIG. 1. Examples of three-field inflation trajectories that can be accurately approximated by an effective model with (a) one, (b) two, and (c) three fields, respectively. For example, the field trajectory in (b) requires more than one effective field to represent the trajectory because it curves, but the trajectory curves only in a plane, so only two effective fields are needed.

cal to test each model against cosmic data. Indeed, we illustrated this point in [13] by examining a few classes of models (for example, double quadratic models) and rigorously testing them by considering the full range of initial conditions. For each type of model, we tested more than 10,000 scenarios by varying both a parameter value in the Lagrangian and the initial conditions, in

order to constrain that class of models using WMAP constraints on the power spectra. But as we demonstrated in [13], such an approach is extremely time-consuming. Instead of testing each inflationary scenario one by one, a more fruitful approach is to determine how key features of multi-field inflationary Lagrangians translate into observable quantities. For example, how is the geometry of the inflationary potential reflected in the cosmic observables? Is there a way to tell from cosmic data whether a one-field or two-field model can fit all measurements, as illustrated in Figure 1, or whether more fields are required? And what is the role of nonstandard kinetic terms in determining the cosmic observables? In this paper, we attempt to answer these and other questions, with our ultimate goal being to understand how cosmic data can constrain the form of the inflationary Lagrangian.

We do this by building on the pioneering work of others. Initial work on understanding the perturbations and power spectra generated by general multi-field inflation was done in [14–28]. The specific case of two-field inflation was treated in [13, 28–40]. Work towards calculating other spectra, such as the bispectrum and trispectrum, in general two-field and multi-field inflation was done by [41–62], among others. Interestingly, while developing generic semianalytic formulas for the spectra from multi-field inflation has received much attention, the sourcing relations among the modes in multi-field models has received less attention. Understanding the sourcing effects is important as they provide the link between the inflationary Lagrangian and the cosmic observables. This lack of attention is at odds with investigations of two-field scenarios, in which the sourcing effects have been treated in detail. Related to the mode sourcing is the effective number of fields needed to describe an inflationary scenario. Knowing the effective number of fields is important because it can lead to dramatic simplifications of the expressions for the spectra and it allows us to focus on the most important features of an inflationary model. For example, if a multi-field model with ten scalar fields behaves like a two-field model during the last several dozen e-folds of inflation, then using this fact greatly enhances our understanding of that model, as well as largely reduces the computational complexity of the spectra.

In this paper, we focus on the underappreciated series of mode sourcing relations and how they are determined by the inflationary Lagrangian, in order to extend our insights from [13, 69] to multi-field inflation. The rest of this paper is organized as follows. In Section II, we cover the dynamics and kinematics of the background fields, and we discuss slow-roll and other limiting cases of behavior. In Section III, we present equations of motion for the field perturbations in both the given and kinematical bases. We then prove that most of the coefficients of the mass matrix vanish in the kinematical basis, and we use this fact to derive a simplified series of sourcing equations for the modes. In tandem, we discuss how the geometric and kinematical features of the inflationary Lagrangian determine the interactions among the modes. Finally,

in Section IV, we use these sourcing equations to examine the effective number of fields in multi-field models and to explore how this number is reflected in spectral observables. We also generalize our two-field semianalytic formulas for the bispectrum and trispectrum [69] to multi-field inflation, introduce a new multi-field consistency condition, and identify a spectral observable that can be used to distinguish two-field models from models with three or more fields. This work paves the way toward a better understanding of how the features of multi-field inflationary Lagrangians are reflected in the cosmic observables.

II. BACKGROUND FIELDS

We start our treatment of multi-field inflation by examining the dynamics and kinematics of the background fields. In Section II A, we review notation and the equation of motion for the background fields. In Section II B, we outline a framework for understanding the field vector kinematics, which is based on work by [13, 21, 23, 30]. We conclude our treatment of the background fields in Section II C by exploring the standard slow-roll limit and other limiting cases of behavior. This extended work-up—particularly on the background kinematics—lays the necessary groundwork for us to connect the geometric features of an inflationary Lagrangian to the cosmic observables.

A. Evolution Equation for the Fields

We consider inflationary scenarios driven by an arbitrary number of scalar fields, ϕ_i , where $i = 1, 2, \dots, d$, and d is the total number of scalar fields present during inflation. Here, we allow for the possibility that some number of the d scalar fields do not contribute to the inflationary expansion. Which of these fields do and do not contribute to the inflationary expansion does not need to be known in advance, as the formalism presented here will automatically take care of this. To represent the fields compactly, we use the notation

$$\phi \equiv (\phi_1, \phi_2, \dots, \phi_d), \quad (1)$$

and we call ϕ the field vector for short, even though the fields do not transform as vectors. Here, we express the fields in units of the reduced Planck mass, $\bar{m} \equiv 1/\sqrt{8\pi G}$, and we work in units where $c = \hbar = \bar{m} = 1$.

Assuming Einstein gravity, we take the non-gravitational part of the inflationary action to be

$$S = \int \left[-\frac{1}{2} g^{\mu\nu} G_{ij} \frac{\partial \phi^i}{\partial x^\mu} \frac{\partial \phi^j}{\partial x^\nu} - V(\phi) \right] \sqrt{-g} d^4x, \quad (2)$$

where $g_{\mu\nu}$ is the spacetime metric and G_{ij} determines the form of the kinetic terms in the Lagrangian. G_{ij} is called the field metric, which we assume is a function of only the

fields, and it can be viewed as inducing a field manifold. If the kinetic terms are canonical, then $G_{ij} = \delta_{ij}$, and the field manifold reduces to Euclidean space. Here, we allow both the field metric and the inflationary potential, $V(\phi)$, to be arbitrary.

Before proceeding, we introduce some notational shorthand. We use Latin indices to represent quantities related to the fields, ϕ_i . For vectorial quantities lying in the tangent and cotangent bundles of the field manifold, we use boldface vector notation and standard inner product notation. The inner product of two vectors \mathbf{A} and \mathbf{B} is

$$\mathbf{A}^\dagger \mathbf{B} \equiv \mathbf{A} \cdot \mathbf{B} \equiv G_{ij} A^i B^j, \quad (3)$$

where we use the symbol † on a naturally contravariant or covariant vector to denote its dual, e.g., $\dot{\phi}^\dagger \equiv (G_{ij} \dot{\phi}^j)$ and $\nabla^\dagger \equiv (G^{ij} \nabla_j)$. Norms are defined as the square root of the inner product of a vector with itself:

$$|\mathbf{A}| \equiv \sqrt{\mathbf{A}^\dagger \mathbf{A}}. \quad (4)$$

Lastly, instead of working in terms of the coordinate time, t , we work in terms of N , which represents the logarithmic growth of the scale factor, $a(t)$:

$$dN \equiv d \ln a = H dt, \quad (5)$$

where $H \equiv \frac{\dot{a}}{a}$ is the Hubble parameter. In other words, N represents the number of e-folds of the scale factor. We work in terms of N because it is dimensionless, it relates to a more physical measure of time, and it simplifies the equations of motion [13, 19]. To denote differentiation with respect to N , we use the notation

$$' \equiv \frac{d}{dN}. \quad (6)$$

We are now ready to present an equation of motion for the fields—the main goal of this section. By imposing covariant conservation of energy, we derived such an equation using N as the time variable in [13]. We found that the equation of motion for the fields can be written as

$$\frac{\eta}{(3 - \epsilon)} + \phi' + \nabla^\dagger \ln V = 0, \quad (7)$$

where

$$\epsilon \equiv -(\ln H)' = \frac{1}{2} \phi' \cdot \phi', \quad (8)$$

and the covariant field acceleration η is defined as

$$\eta \equiv \frac{D\phi'}{dN}. \quad (9)$$

The symbol D acting on a contravariant vector X^i means

$$DX^i \equiv d\phi^j \nabla_j X^i = d\phi^j (\partial_j X^i + \Gamma_{jk}^i X^k), \quad (10)$$

where Γ_{jk}^i and ∇_j are the Levi-Civita connection and the covariant derivative, respectively, associated with the field metric. Therefore, η represents the covariant rate of change of the field velocity vector with respect to the field manifold—that is, it represents deviations from perfect parallel transport of ϕ' . By working in terms of D and the covariant derivative ∇ , we are able to write all the equations of motion in manifestly covariant form.

B. Field Vector Kinematics

The kinematics of the background fields are important because they allow us to follow how the geometric features of an inflationary Lagrangian translate into values for the spectral observables. Conversely, experimental bounds on spectral observables often translate into constraints on the background kinematics, which in turn constrain the inflationary Lagrangian. In other words, the field kinematics serve as intermediaries between the inflationary Lagrangian and the spectral observables. We discussed this in great detail for the case of general two-field inflation with noncanonical kinetic terms in [13]. Here, we extend that and other work by presenting a kinematical framework for the general case of multi-field inflation.

The first kinematical framework for multi-field inflation was constructed by [30] for the specific case of two-field inflationary potentials with canonical kinetic terms. Soon after, Nibbelink and Van Tent extended this framework to describe multi-field inflation with noncanonical kinetic terms [21, 23]. In [13], we slightly modified this framework in applying it to two-field inflation with noncanonical kinetic terms. Here, we combine elements from [13, 21, 23] in presenting a kinematical framework for multi-field inflation. We will note where any quantities we introduce are different from those originally proposed by Nibbelink and Van Tent.

To construct a kinematical framework, we start in the normal manner by considering the velocity, acceleration, and higher-order derivatives of the coordinates. Here, the coordinates are the scalar fields, which represent the coordinate position on the manifold induced by the field metric. In analogy to Newtonian mechanics, ϕ represents the position, ϕ' is the velocity, and $\eta \equiv \frac{D\phi'}{dN}$ represents the covariant acceleration, where $\frac{D}{dN}$ is effectively defined by Eq. (10). Similarly, we can define higher-order covariant derivatives of the field velocity ad infinitum. The jerk is defined as

$$\xi \equiv \frac{D^2 \phi'}{dN^2}. \quad (11)$$

And an equation of motion for the jerk can be obtained by differentiating Eq. (7) once, which yields

$$\frac{\xi}{(3 - \epsilon)} + \eta = - \left[\mathbf{M} + \frac{\eta \eta^\dagger}{(3 - \epsilon)^2} \right] \phi', \quad (12)$$

where the *mass matrix*, \mathbf{M} , is defined as

$$\mathbf{M} \equiv \nabla^\dagger \nabla \ln V \quad (13)$$

and is symmetric. Similarly, we represent the $(n-1)$ -th covariant derivative of the velocity by the notation

$$\chi^{(n)} = \left(\frac{D}{dN} \right)^{(n-1)} \phi', \quad (14)$$

and an equation of motion for $\chi^{(n)}$ can be obtained by differentiating Eq. (7) a total of $n-2$ times. For comparison, Nibbelink and Van Tent [23] defined a series of higher-order kinematical vectors as

$$\tilde{\eta}^{(n)} \equiv \frac{\mathcal{D}^{(n-1)} \phi^i}{\left(\frac{a^i}{a} \right)^{(n-1)} |\phi^i|}, \quad (15)$$

where $\dot{}$ represents the derivative with respect to the arbitrary time variable τ and \mathcal{D} is the “slow-roll derivative”.¹ Both constructs have their utility: Nibbelink and Van Tent’s construct makes their vectors manifestly independent of the choice of time coordinate, while our construct is more physically intuitive and can be used to simplify many inflationary expressions to a greater degree.

To accompany these kinematical vectors, one can construct a basis that is induced by the field vector kinematics. Working in this basis simplifies the equations of motion for the field perturbations. In [13], we dubbed this kinematically-induced basis the *kinematical basis*. Gordon et al. [30] first developed such a basis for two-field inflation with canonical kinetic terms, and Nibbelink and Van Tent extended this basis to multi-field inflation with noncanonical kinetic terms [21, 23]. In [13], we adopted this same basis, but used N as the time variable when we applied it to two-field inflation with noncanonical kinetic terms. The construction of this basis is as follows. The first basis vector, \mathbf{e}_1 , is chosen to lie in the direction of the field velocity, so that it is parallel to the field trajectory. The second basis vector, \mathbf{e}_2 , is constructed to lie along the part of the field acceleration that is orthogonal to the field velocity, in the direction that makes $\mathbf{e}_2 \cdot \boldsymbol{\eta} \geq 0$. Using the Gram-Schmidt orthogonalization procedure, this process is continued until there are d basis vectors. In

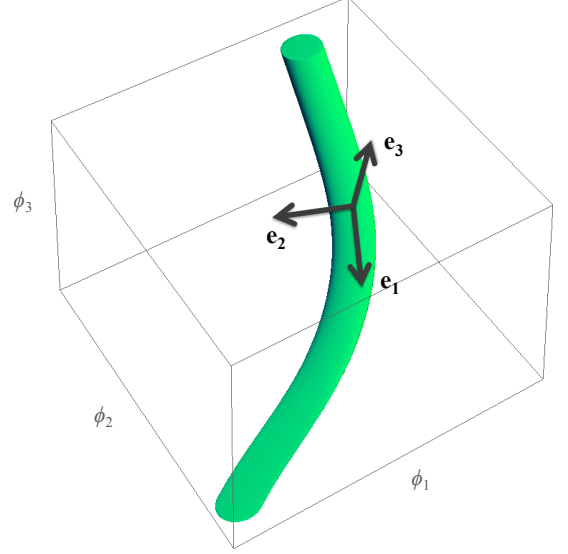


FIG. 2. An example showing how the kinematical basis is constructed from the kinematics of the background fields. The green curved path represents the trajectory of the field vector in a three-field inflation scenario, as a function of the time variable N . At each point on the trajectory, the \mathbf{e}_1 basis vector is chosen to point in the direction of the field velocity, \mathbf{e}_2 points in the direction of the perpendicular acceleration, and \mathbf{e}_3 is constructed to be orthogonal to the first two basis vectors.

other words, the kinematical basis vectors are

$$\begin{aligned} \mathbf{e}_1 &\equiv \frac{\phi'}{|\phi'|} \\ \mathbf{e}_2 &\equiv \frac{(\mathbf{I} - \mathbf{e}_1 \mathbf{e}_1^\dagger) \boldsymbol{\eta}}{|(\mathbf{I} - \mathbf{e}_1 \mathbf{e}_1^\dagger) \boldsymbol{\eta}|} \\ &\dots \\ \mathbf{e}_d &\equiv \frac{\left(\mathbf{I} - \sum_{i=1}^{d-1} \mathbf{e}_i \mathbf{e}_i^\dagger \right) \chi^{(d)}}{\left| \left(\mathbf{I} - \sum_{i=1}^{d-1} \mathbf{e}_i \mathbf{e}_i^\dagger \right) \chi^{(d)} \right|}, \end{aligned} \quad (16)$$

where \mathbf{I} is the appropriate identity matrix. Now, if the kinematical vector $\chi^{(n)}$ already lies in the subspace defined by the basis vectors $\mathbf{e}_1, \mathbf{e}_2, \dots, \mathbf{e}_{n-1}$, then it is not possible to find a projection of $\chi^{(n)}$ that represents a new direction in field space. In this case, \mathbf{e}_n can simply be constructed at will so that it represents a new direction that is orthogonal to the subspace spanned by the basis vectors \mathbf{e}_1 through \mathbf{e}_{n-1} , and then the orthogonalization process can naturally proceed again. Our basis vectors are effectively identical to those of Nibbelink and Van Tent [21, 23], despite our different definition for the kinematical vectors.

With these basis vectors, we can take projections of vectors and matrices. For example,

$$\chi_n^{(m)} \equiv \mathbf{e}_n \cdot \chi^{(m)} \quad (17)$$

¹ The “slow-roll derivative” is defined as $\mathcal{D}(b^n A) \equiv \left(\frac{D}{d\tau} - n \frac{d \ln b}{d\tau} \right) (b^n A)$, where $b = -g_{00}$ and A is independent of b . Our kinematical vectors differ from Nibbelink and Van Tent’s in two ways: (1) the effective order in the slow-roll expansion, which differs because of the factor of $|\phi^i|$ in the denominator in Eq. (15), and (2) the expressions themselves—that is, our series differs from theirs even when the order of Eq. (15) is adjusted by multiplying by $|\phi^i|$. For more information, we refer the interested reader to [23].

represents the projection of the kinematical vector $\chi^{(m)}$ onto the basis vector \mathbf{e}_n . Note that because of the definition of the kinematical basis vectors in Eq. (16), if $n > m$, then $\chi_n^{(m)} = 0$. That is, in the kinematical basis, ϕ' has the sole nonzero component

$$v \equiv |\phi'|; \quad (18)$$

η has nonzero components η_1 and η_2 ; ξ has nonzero components ξ_1 , ξ_2 , and ξ_3 ; and so on. The projection of any vector along \mathbf{e}_1 is particularly noteworthy, as it represents the vector component parallel to the field trajectory. To extend these projections to any matrix \mathbf{A} , we use the shorthand notation

$$A_{mn} \equiv \mathbf{e}_m^\dagger \mathbf{A} \mathbf{e}_n \quad (19)$$

for the matrix coefficients and

$$\mathbf{A}_{\perp\perp} \equiv (\mathbf{I} - \mathbf{e}_1 \mathbf{e}_1^\dagger) \mathbf{A} (\mathbf{I} - \mathbf{e}_1 \mathbf{e}_1^\dagger) \quad (20)$$

for the above special matrix projection.

The last useful part of this kinematical framework is the derivatives of the basis vectors with respect to the number of e-folds of inflation, N . These temporal derivatives represent how quickly the basis vectors are covariantly changing direction with respect to the field manifold. In particular, the derivative of the basis vector parallel to the field velocity, \mathbf{e}_1 , represents how quickly the field trajectory itself is covariantly changing direction. It is given by differentiating Eq. (16), which yields

$$\frac{D\mathbf{e}_1}{dN} = \frac{\eta_2}{v} \mathbf{e}_2. \quad (21)$$

Similarly, differentiating the second basis vector gives

$$\frac{D\mathbf{e}_2}{dN} = \frac{\xi_3}{\eta_2} \mathbf{e}_3 - \frac{\eta_2}{v} \mathbf{e}_1. \quad (22)$$

The derivative of the n th basis vector is

$$\frac{D\mathbf{e}_n}{dN} = \frac{\chi_{n+1}^{(n+1)}}{\chi_n^{(n)}} \mathbf{e}_{n+1} - \frac{\chi_n^{(n)}}{\chi_{n-1}^{(n-1)}} \mathbf{e}_{n-1}. \quad (23)$$

Thus, another benefit of the kinematical basis is that when the \mathbf{e}_n basis vector changes direction, it can pick up components along only the \mathbf{e}_{n-1} and \mathbf{e}_{n+1} directions. Furthermore, because $\frac{D}{dN}(\mathbf{e}_{n+1} \cdot \mathbf{e}_n) = 0$, we have the relation [23]

$$\mathbf{e}_{n+1} \cdot \frac{D\mathbf{e}_n}{dN} = -\frac{D\mathbf{e}_{n+1}}{dN} \cdot \mathbf{e}_n. \quad (24)$$

Hence, the matrix

$$Z_{mn} \equiv \mathbf{e}_m \cdot \frac{D\mathbf{e}_n}{dN} \quad (25)$$

is skew-symmetric with the only nonzero components being

$$Z_{n+1,n} = -Z_{n,n+1} = \frac{\chi_{n+1}^{(n+1)}}{\chi_n^{(n)}}. \quad (26)$$

The \mathbf{Z} matrix therefore encodes how quickly the d basis vectors are changing direction. For comparison, we note that the derivatives of the basis vectors and the \mathbf{Z} matrix are equivalent to those in [23], even though we defined the kinematical vectors differently.

Lastly, we compare \mathbf{Z} when there are one, two, and three or more fields present during inflation. In single-field inflation, there is only one basis vector and this basis vector cannot change direction, so \mathbf{Z} reduces to the zero matrix. In two-field inflation, the only nonzero coefficients of \mathbf{Z} are $Z_{21} = -Z_{12} = \frac{\eta_2}{v}$, and so only this single quantity is needed to characterize how quickly both basis vectors are covariantly changing direction.² In [13], we called this quantity the *turn rate*, since it represents how quickly the background field trajectory is turning with respect to the field manifold. However, for multi-field inflation with three or more fields, there are multiple such rates that characterize how quickly the d basis vectors are rotating. Therefore, to extend our two-field formalism to multi-field inflation, we call $|\frac{D\mathbf{e}_n}{dN}|$ the *turn rate for the n th basis vector*, and we say that the kinematical quantity $Z_{n+1,n}$ represents how quickly the \mathbf{e}_n basis vector is turning into the direction of \mathbf{e}_{n+1} . Because \mathbf{Z} summarizes the turn rates for all basis vectors, we call \mathbf{Z} the *turn rate matrix*. The turn rate matrix is therefore the multi-field generalization of the idea of a single covariant turn rate for two-field inflation. The turn rate matrix, along with the kinematical basis vectors, plays a key role in determining the dynamics of the field perturbations.

C. Slow-Roll And Other Limits

Having delineated a framework to represent the kinematics of any multi-field model, we now consider the slow-roll limit and other special subcases of limiting behavior that simplify the equations of motion.

In standard single-field inflation, the slow-roll limit is invoked in order to guarantee nearly exponential expansion of the scale factor, which produces a nearly scale-invariant density power spectrum. In this limit, the field is slowly rolling, which effectively means that both the field speed and field acceleration are small, satisfying $\eta \ll \phi' \ll 1$. (Recall that we constructed both the field velocity and field acceleration to be dimensionless.) The slow-roll limit implies that the field acceleration is negligible in Eq. (7), which allows us to simplify the equations of motion and obtain analytic estimates for the power spectrum and spectral observables.

In multi-field inflation, an analogous slow-roll limit is typically defined by the two conditions (e.g., [29, 32, 33,

² In [13], we wrote the quantity $\frac{\eta_2}{v}$ as $\frac{\eta_\perp}{v}$ since in two-field inflation, there is only a single direction perpendicular to the field trajectory.

35, 36]):

$$\epsilon \approx \frac{1}{2} |\nabla \ln V|^2 \ll 1, \quad (27)$$

$$|M_{ij}| \ll 1. \quad (28)$$

In some approaches (e.g., [19, 21, 23]), the second condition above is effectively replaced by the condition

$$\eta \ll \phi' \quad (29)$$

in our notation. We examined these conditions in the case of two-field inflation, the simplest case of multi-field inflation, in [13]. As a result of that analysis, we argued for a more nuanced approach to the slow-roll approximation that splits the slow-roll limit into two separate limits—the slow-roll limit and the slow-turn limit. Our redefined slow-roll limit corresponds to the conditions

$$\begin{aligned} \epsilon &\ll 1, \\ \left| \frac{\eta_1}{v} \right| &\ll 1, \end{aligned} \quad (30)$$

which means that the field speed and the rate at which the field speed is logarithmically changing are small. This redefined slow-roll limit corresponds to limits on single-field-like behavior. In contrast, our two-field slow-turn limit in [13] corresponds to what can be viewed as distinctly multi-field behavior. It corresponds to limits on how quickly the field trajectory is covariantly changing direction—a distinctly multi-field behavior—and it can be expressed as

$$\left| \frac{D\mathbf{e}_1}{dN} \right| = \frac{\eta_2}{v} = Z_{21} \ll 1. \quad (31)$$

The power of distinguishing between the rolling and turning behaviors of the field vector is that they have very different effects on the density power spectrum, and different approximations can be made depending on whether the field velocity is slowly rolling, slowly turning, or both.

Here, we extend this more nuanced approach for two-field inflation to general multi-field inflation. First, we will refer to the redefined slow-roll limit—the limits on single-field-like behavior, as defined by Eq. (30)—as the *single-field slow-roll limit*. Second, to extend the slow-turn formalism to multi-field inflation, we say that a basis vector \mathbf{e}_n is slowly turning if

$$\left| \frac{D\mathbf{e}_n}{dN} \right| \ll 1, \quad (32)$$

and also say that the corresponding scenario is in the \mathbf{e}_n *slow-turn limit*. By Eq. (23), if $\chi_{n-1}^{(n-1)}$, $\chi_n^{(n)}$, and $\chi_{n+1}^{(n+1)}$ are all nonzero, then Eq. (32) is equivalent to the requirement that $\chi_{n-1}^{(n-1)} \gg \chi_n^{(n)} \gg \chi_{n+1}^{(n+1)}$. When all d basis vectors are slowly turning, we say that the inflationary scenario is in the *slow-turn limit*, and the magnitude of every component of the turn rate matrix, \mathbf{Z} , is significantly less than one. For reasons that will become

more apparent later, the full slow-turn limit represents limits on multi-field behavior; this is because the turn rates play a critical role in determining the interactions among modes in the kinematical basis.

Taken together, the single-field slow-roll limit and the slow-turn limit constitute our two main *kinematical limits* of interest. However, in investigating the modes in the kinematical basis, we will want to invoke not just these two limits but also the limit in Eq. (28) to ensure that the acceleration term in the mode equations can be neglected. When we combine these three limits together, we call the combined limit simply the *slow-roll limit*, even though we are also assuming full slow-turn behavior. We do this to avoid introducing new nomenclature that would create confusion with past literature. In this paper, we focus on the full slow-roll limit, but we introduce the above separate limits so that different individual limits can be explored, like we did for two-field inflation in [13]. For example, by exploring these separate limits in [13], we found that two-field models that strongly violate the slow-turn limit around horizon-crossing but not the single-field slow roll limit are ruled out by WMAP constraints on the power spectrum. We emphasize that much is to gain from a similar thorough investigation of multi-field inflation, and this paper lays much of the foundation for such an investigation.

Now we are ready to apply the above set of limits to the background equations of motion and our kinematical vectors to simplify them. Eq. (7) for the evolution of the fields reduces to

$$\phi' \approx -\nabla^\dagger \ln V \quad (33)$$

whenever the single-field slow-roll and the \mathbf{e}_1 slow-turn limits hold; the full slow-roll limit does not need to be invoked. Rotating to the kinematical basis, in the single-field slow-roll and \mathbf{e}_1 slow-turn limits, the field speed is given by

$$v \approx |\nabla \ln V|, \quad (34)$$

or equivalently by

$$\epsilon \approx \frac{1}{2} |\nabla \ln V|^2. \quad (35)$$

Also under the same two limits, by virtue of Eq. (33), the operator $\frac{D}{dN} = \phi' \cdot \nabla$ becomes

$$\frac{D}{dN} \approx -\nabla \ln V \cdot \nabla. \quad (36)$$

Using this expression, the kinematical vectors in the full slow-roll limit can be approximated by

$$\chi^{(n)} \approx (-\nabla \ln V \cdot \nabla)^{(n-1)} (-\nabla^\dagger \ln V). \quad (37)$$

For example,

$$\eta \approx -\mathbf{M}\phi' \approx \mathbf{M}\nabla^\dagger \ln V, \quad (38)$$

and

$$\begin{aligned}\xi &\approx -\mathbf{M}\eta - \frac{D\mathbf{M}}{dN}\phi' \\ &\approx -[\mathbf{M}^2 + (\nabla \ln V \cdot \nabla \mathbf{M})] \nabla^\dagger \ln V.\end{aligned}\quad (39)$$

The slow-roll approximations for the kinematical basis vectors follow directly from the above results, with Eq. (37) substituted for $\chi^{(n)}$ in Eq. (16). For example, in the slow-roll approximation,

$$\begin{aligned}\mathbf{e}_1 &\approx -\frac{\nabla^\dagger \ln V}{|\nabla \ln V|}, \\ \mathbf{e}_2 &\approx \left[\mathbf{I} - \frac{\nabla^\dagger \ln V}{|\nabla \ln V|} \left(\frac{\nabla \ln V}{|\nabla \ln V|} \right) \right] \mathbf{M} \nabla^\dagger \ln V,\end{aligned}\quad (40)$$

and so on.

These results will be very important in simplifying the equations of motion and the interactions among modes in multi-field inflation.

III. FIELD PERTURBATIONS

Now we consider the field perturbations during inflation. First, we present equations of motion for the field perturbations in Section III A. We provide evolution equations in both the given and kinematical bases. In Section III B, we explore the properties of the mass matrix, showing for the first time that most of its coefficients vanish in the kinematical basis. We use this result in Section III C to show that the interactions among modes greatly simplify in the kinematical basis. We then analyze these mode interactions and discuss how they depend on the geometric features of multi-field inflationary Lagrangians and their associated field trajectories. This section lays the key foundation that allows us to connect the geometric features of inflationary Lagrangians to the cosmic observables.

A. Evolution Equations for the Field Perturbations

In this section, we present equations of motion for the field perturbations. In doing so, we work in the flat gauge, and we do this for two reasons. First, in this gauge, the field perturbations decouple from the metric perturbations. Second, the field vector perturbation in the flat gauge turns out to be the gauge-invariant Mukhanov-Sasaki variable, $\delta\phi_f = \delta\phi + \psi\phi'$, where ψ represents the scalar metric perturbation on spatial hypersurfaces [63, 64]. From here forward, since we consider the perturbations only in the flat gauge, we drop the subscript f from $\delta\phi_f$.

We derive an equation for the field perturbations in the given basis by imposing covariant conservation of energy to first order in the field perturbations, as has been done

before [17, 18, 21]. However, instead of the standard approach, we use N as the time variable, both because it is more physically intuitive and it makes the equation of motion dimensionless. We derived such an equation in the context of general two-field inflation with noncanonical kinetic terms in [13]. Following the same series of steps, we arrive at the same expression, with the exception that the curvature term arising from the field metric is a matrix in general multi-field inflation.³ The resulting equation in Fourier space is

$$\begin{aligned}\frac{1}{(3-\epsilon)} \frac{D^2 \delta\phi}{dN^2} + \frac{D\delta\phi}{dN} + \left(\frac{k^2}{a^2 V} \right) \delta\phi \\ = - \left[\tilde{\mathbf{M}} + \frac{\eta\eta^\dagger}{(3-\epsilon)^2} \right] \delta\phi,\end{aligned}\quad (41)$$

where k is the comoving wavenumber. The term $\tilde{\mathbf{M}}$ is the *effective mass matrix*,⁴ and we define it as

$$\tilde{\mathbf{M}} \equiv \mathbf{M} - \frac{1}{(3-\epsilon)} \mathbf{R},\quad (42)$$

and the curvature matrix, \mathbf{R} , is defined as [21]

$$R^a_d \equiv 2\epsilon R^a_{bcd} e_1^b e_1^c,\quad (43)$$

where R^a_{bcd} is the Riemann curvature tensor associated with the field metric. Because of the symmetry and anti-symmetry properties of the Riemann curvature tensor, it follows that \mathbf{R} is symmetric. Moreover, $\mathbf{R}\phi' = 0$, and hence $\mathbf{R} = \mathbf{R}_{\perp\perp}$.

Next, we consider various limits of Eq. (41). In the superhorizon limit, when the modes are significantly outside the horizon such that $(\frac{k}{aH})^2 \ll 1$, the subhorizon term $(\frac{k^2}{a^2 V}) \delta\phi$ can be neglected. In the combined single-field slow-roll and \mathbf{e}_1 slow-turn limits, we argued in [13] that the term $\frac{\eta\eta^\dagger}{(3-\epsilon)^2}$ can be neglected in two-field inflation since this term is much smaller than $\tilde{\mathbf{M}}$. The exact same arguments as in [13] hold for general multi-field inflation with an arbitrary number of fields. And, whenever both the superhorizon limit and the full slow-roll limit apply, it can be shown [23, 65] that the acceleration of the field perturbations can also be neglected. In these combined limits, Eq. (41) reduces to⁵

$$\frac{D\delta\phi}{dN} \approx -\tilde{\mathbf{M}}\delta\phi.\quad (44)$$

³ For comparison, in two-field inflation, the curvature term effectively reduces to a single degree of freedom: the Ricci scalar (times a scaled outer product of two kinematical basis vectors).

⁴ In comparison to our dimensionless definition of the effective mass matrix, Nibbelink and Van Tent defined the effective mass matrix as $\tilde{\mathbf{M}}^2 \equiv \nabla \nabla^\dagger V - H^2 \mathbf{R}$ [23].

⁵ Technically, Eq. (44) also assumes that the dimensionless components of \mathbf{R} are much less than one.

Let us consider the above superhorizon, slow-roll equation of motion in the kinematical basis. In the kinematical basis, there are up to d nonzero field perturbations, and the n th mode is

$$\delta\phi_n \equiv \mathbf{e}_n \cdot \delta\phi. \quad (45)$$

The benefit of working in the kinematical basis is that it allows us to separate out the adiabatic mode from the entropy modes. The adiabatic or density mode corresponds to $\delta\phi_1$, meaning that it corresponds to the component of $\delta\phi$ that is parallel to the field trajectory. The remaining components of $\delta\phi$ in the kinematical basis correspond to entropy modes. Entropy modes are linear combinations of the field perturbations that leave the overall density unperturbed. As there are d fields in the system, there will be $d - 1$ entropy modes, all of which are orthogonal to the field trajectory and to each other.

Now the equation of motion assumes a different form in the kinematical basis because the basis vectors can rotate, causing the equation of motion (41) to pick up extra terms that trivially vanish in the original given basis. Using the fact that

$$\delta\phi'_n = \mathbf{e}_n \cdot \delta\phi' - \mathbf{e}_n^\dagger \mathbf{Z} \delta\phi, \quad (46)$$

it follows that the corresponding equation in the kinematical basis is

$$\frac{D\delta\phi}{dN} \approx - [\tilde{\mathbf{M}} + \mathbf{Z}] \delta\phi. \quad (47)$$

Note that the term in brackets is the sum of a symmetric matrix and an anti-symmetric matrix. If, however, we are interested in just the evolution of the $d - 1$ entropy modes in the kinematical basis, their equation of motion in the combined superhorizon and slow-roll limits is

$$\frac{D\delta\phi_\perp}{dN} \approx - [\tilde{\mathbf{M}}_{\perp\perp} + \mathbf{Z}_{\perp\perp}] \delta\phi_\perp, \quad (48)$$

where the special matrix projection was defined in Eq. (20). Therefore, if we want to determine the evolution of only the entropy modes, we can study them by reducing the dimension of the perturbed equation of motion by one.

B. Properties of the Mass Matrix

In general, the interactions among modes are most easily understood in the kinematical basis. First, in this basis, the density mode can be teased out from the $d - 1$ entropy modes. Second, it turns out that most of the coefficients of the mass matrix vanish in this basis. This second fact profoundly simplifies the interactions among modes, as we will demonstrate in the following section.

But first, in this section, we prove our claim that most of the coefficients of \mathbf{M} vanish in the kinematical basis. We start from the full equation of motion for the fields

(7). Projecting this equation onto the basis vectors gives $\mathbf{e}_n \cdot \nabla \ln V = 0$ for $n > 2$, since in the kinematical basis, $\boldsymbol{\eta}$ has nonzero components along only \mathbf{e}_1 and \mathbf{e}_2 . Continuing, we differentiate the equation of motion for the fields to obtain Eq. (12) for the jerk, $\boldsymbol{\xi}$. Projecting this equation onto the basis vectors gives $M_{1n} = 0$ for $n > 3$, since $\boldsymbol{\xi}$ has nonzero components along only \mathbf{e}_1 , \mathbf{e}_2 , and \mathbf{e}_3 . Similarly, repeatedly differentiating Eq. (7) and projecting the result onto the basis vectors allows us to find the coefficients of \mathbf{M} and its covariant derivatives that vanish. In the end, we find that

$$M_{mn} = 0 \quad \text{for } |m - n| > 2, \\ \left[\left(\frac{D}{dN} \right)^p \mathbf{M} \right]_{mn} = 0 \quad \text{for } |m - n| > p + 2. \quad (49)$$

The second condition above implies that the vector formed from contracting $\nabla^n V$ with $n - 1$ instances of ϕ' vanishes along the \mathbf{e}_m direction, where $m > n + 1$. This shows that most of the coefficients of \mathbf{M} vanish in the kinematical basis.

In the full slow-roll limit, the mass matrix simplifies even further. The proof is similar to the above proof for the general case, except we start with the slow-roll equation of motion (33). Projecting this equation onto the basis vectors trivially gives that $\mathbf{e}_n \cdot \nabla \ln V = 0$ for $n > 1$. Differentiating the slow-roll equation of motion once and projecting it onto the basis vectors gives $M_{1n} = 0$ for $n > 2$. Similarly, repeatedly differentiating Eq. (33), we obtain

$$\chi^{(n+2)} \approx - \sum_{m=0}^n \binom{n}{m} \left[\left(\frac{D}{dN} \right)^m \mathbf{M} \right] \chi^{(n-m+1)}. \quad (50)$$

Projecting Eq. (50) onto the kinematical basis vectors gives

$$M_{mn} \approx 0 \quad \text{for } |m - n| > 1, \\ \left[\left(\frac{D}{dN} \right)^p \mathbf{M} \right]_{mn} \approx 0 \quad \text{for } |m - n| > p + 1. \quad (51)$$

Therefore, in the full slow-roll limit, \mathbf{M} reduces even further and becomes a symmetric tridiagonal matrix in the kinematical basis. This concludes our proofs showing that most of the coefficients of the mass matrix do indeed vanish in the kinematical basis.

C. Mode Sourcing Equations

Our goals in the rest of Section (III) are two-fold: to simplify the equations of motion as much as possible and to gain intuition and physical insight into the mode interactions. Doing so will bring us much closer to our ultimate goal of connecting the geometric and kinematical features arising from the inflationary Lagrangian with the cosmic observables.

In exploring the interactions among modes, we consider the superhorizon equation of motion for each of the d modes in the kinematical basis. When a mode $\delta\phi_m$ affects the evolution of mode $\delta\phi_n$, we say that $\delta\phi_m$ *sources* $\delta\phi_n$, regardless of whether that interaction causes $\delta\phi_n$ to increase or decrease in amplitude. And we call the interaction between the two modes a *sourcing relationship*. Since we will group all sourcing terms on the right-hand side of each equation, we refer to such equations as *mode sourcing equations*. Surprisingly, studying the interactions among modes one by one like this has not received much attention in general multi-field inflation; however, studies have been undertaken concerning the adiabatic mode in multi-field inflation (in particular, [21, 23]) and in general two-field inflation [13, 29–40]. Here we fill this important gap in the literature.

We start with the mode sourcing equation for the adiabatic mode, $\delta\phi_1$, which is most easily derived from the fact that the comoving density perturbation vanishes in the superhorizon limit. Imposing this constraint yields [13, 23, 30]

$$\left(\frac{\delta\phi_1}{v}\right)' = 2\frac{D\mathbf{e}_1}{dN} \cdot \frac{\delta\phi}{v} = 2Z_{21}\left(\frac{\delta\phi_2}{v}\right). \quad (52)$$

In the slow-roll limit, the above equation can be written as

$$\delta\phi_1' + M_{11}\delta\phi_1 \approx 2Z_{21}\delta\phi_2, \quad (53)$$

where we have used that $Z_{21} \approx -M_{12}$, which follows from Eqs. (21), (38), and (52). Examining Eq. (52) reveals that the adiabatic mode is sourced only when

the field trajectory changes direction with respect to the field manifold (e.g., [3, 13, 21, 23, 30]). The strength of the sourcing depends on the \mathbf{e}_1 turn rate, so in our kinematical picture, the faster the background trajectory changes direction, the more the adiabatic density mode grows.⁶ Moreover, the adiabatic mode can be sourced only by the entropy mode $\delta\phi_2$; none of the other modes can source the adiabatic mode. Otherwise, when the field trajectory does not turn or $\delta\phi_2$ vanishes, it follows that $\delta\phi_1 \propto v$, which is tantamount to single-field behavior.

Continuing, for each of the entropy modes, we can also derive a mode sourcing equation. Here we present the results only for the slow-roll limit, as the full equations of motion are significantly more cumbersome without offering much additional insight, and moreover, they are usually not needed. For the $d-1$ entropy modes, we can derive slow-roll approximations to the sourcing equations starting from Eq. (47) and using Eq. (51). For the $\delta\phi_2$ mode, we obtain

$$\delta\phi_2' + \tilde{M}_{22}\delta\phi_2 \approx -(\tilde{M}_{23} - Z_{32})\delta\phi_3 + \frac{1}{3}\sum_{m=4}^d R_{2m}\delta\phi_m, \quad (54)$$

where we have again used that $Z_{21} \approx -M_{12}$. First, notice that the adiabatic mode does not source the $\delta\phi_2$ mode; in fact, the adiabatic mode does not source any of the entropy modes in the superhorizon limit (regardless of whether the slow-roll limit applies). Second, if the kinetic terms are canonical, then \mathbf{R} vanishes, and $\delta\phi_2$ can be sourced only by $\delta\phi_3$. Conversely, $\delta\phi_2$ will be sourced by the $\delta\phi_n$ mode whenever $R_{2n} \neq 0$. Similarly, for the $\delta\phi_n$ mode, where $n \geq 3$, the sourcing equation is

$$\delta\phi_n' + \tilde{M}_{nn}\delta\phi_n \approx -(\tilde{M}_{n,n-1} + Z_{n,n-1})\delta\phi_{n-1} - (\tilde{M}_{n,n+1} - Z_{n+1,n})\delta\phi_{n+1} + \frac{1}{3}\sum_{m=2, |n-m|>1}^d R_{nm}\delta\phi_m. \quad (55)$$

Importantly, the coefficients of the mass and turn rate matrices allow $\delta\phi_n$ to be sourced by only two modes: $\delta\phi_{n-1}$ and $\delta\phi_{n+1}$.⁷ If the kinetic terms are noncanonical, the other entropy modes $\delta\phi_m$ can source $\delta\phi_n$ only if

$R_{nm} \neq 0$ is satisfied. These results are tantamount to reducing the complexity of the matrix equation (47) by recognizing that the sum $\mathbf{M} + \mathbf{Z}$ is a tridiagonal matrix in the kinematical basis and by recognizing that $M_{12} = -Z_{21}$.

These novel results show that the sourcing equations for the modes profoundly simplify in the kinematical basis, which will allow us to better understand and more easily calculate the interactions among modes.

1. Connections between the mode sourcing and the geometry and kinematics of inflation

Now we analyze the connections between the mode sourcing and the geometry and kinematics of inflation.

⁶ In the classical treatment of Eq. (52), this statement is implied to be taken with respect to assuming that $\delta\phi_1$ and $\delta\phi_2$ are both positive. In the quantum treatment, when we speak of the mode $\delta\phi_1$ growing, it is implied that we are referring to the variance of $\delta\phi_1$ growing. Similar assumptions are made when discussing the other modes.

⁷ For comparison, in the non-slow-roll case (results not shown), up to four modes ($\delta\phi_{n-2}$, $\delta\phi_{n-1}$, $\delta\phi_{n+1}$, and $\delta\phi_{n+2}$) can source $\delta\phi_n$ when the kinetic terms are canonical. This follows directly from the special form of the mass matrix in the kinematical basis, which we covered in the previous section.

First, consider what happens in the absence of sourcing. For $\delta\phi_n$ to be unsourced, Eqs. (53)-(55) show that \mathbf{e}_n must not be turning and the mass matrix coefficients $M_{n,n+1}$ and $M_{n,n-1}$ must vanish, as well as the curvature matrix coefficients R_{nm} for all $m \neq n$ (or when the sourcing terms in aggregate sum to zero). When these conditions are met, the $\delta\phi_n$ mode is unsourced and obeys⁸

$$\delta\phi_n \propto e^{-\int \tilde{M}_{nn} dN}. \quad (56)$$

That is, the *effective mass for the n th mode*, \tilde{M}_{nn} , determines that mode's intrinsic evolution rate.⁹

The effective mass depends on the covariant Hessian of the inflationary potential, $M_{nn} \equiv \nabla_n \nabla_n \ln V$, and on the curvature tensor of the field manifold. Since these are both geometric quantities, this means that we can predict the behavior of $\delta\phi_n$ simply by determining the geometric features of the Lagrangian. For instance, when the potential $\ln V$ is “concave up” along the \mathbf{e}_n direction—that is, when the Hessian coefficient $\nabla_n \nabla_n \ln V$ is positive—this causes $\delta\phi_n$ to decay. Conversely, if the potential has a concave down shape along the \mathbf{e}_n direction, this causes $\delta\phi_n$ to grow. A well-known example exhibiting this behavior is the adiabatic mode in single-field inflation, which is often likened to a ball rolling down a hill that speeds up or slows down depending on the ground's concavity. A second good example is the $\delta\phi_2$ mode in two-field inflation with canonical kinetic terms; if the two-dimensional field trajectory is rolling in a valley (concave up), then the $\delta\phi_2$ mode decays, but if it is rolling along a hill (concave down), then $\delta\phi_2$ grows in amplitude.

The second geometrical quantity, the curvature term R_{nn} , is a bit more complicated to understand. It involves the contraction of the Riemann tensor of the field metric with two instances each of \mathbf{e}_1 and \mathbf{e}_n . Geometrically, it represents 2ϵ times the \mathbf{e}_n component of the failure of \mathbf{e}_1 to be parallel-transported around a closed loop defined by the directions \mathbf{e}_1 and \mathbf{e}_n . Therefore, its contribution to the mode sourcing can in principle be determined from the geometry of the field metric and the potential. If this deviation from parallel transport of \mathbf{e}_1 results in a positive component along the \mathbf{e}_n direction, then this causes $\delta\phi_n$ to grow; conversely, a negative value causes $\delta\phi_n$ to decay. For example, in two-field inflation, since R_{22} is proportional to negative ϵ times the Ricci scalar of the field manifold, if the field manifold is locally elliptical, this will cause $\delta\phi_2$ to decay, while a locally hyperbolic

surface will cause $\delta\phi_2$ to grow (see [13]). Note that if both M_{nn} and R_{nn} have the same sign, they will partially negate each other; thus, it is their net effect that matters. Therefore, we can view the effective mass as some sort of measure of the “net curvature” or geometry of the inflationary Lagrangian along the single direction specified by \mathbf{e}_n . And the steeper this net curvature of the Lagrangian along the \mathbf{e}_n direction, the faster the mode $\delta\phi_n$ evolves.

The corollary of Eq. (56) is that when $\delta\phi_n$ is unsourced, the quantity

$$\delta\phi_n e^{\int \tilde{M}_{nn} dN} \quad (57)$$

is conserved in the superhorizon limit. For example, in single-field inflation, the $\delta\phi_1$ mode is automatically unsourced, and hence the quantity

$$\delta\phi_1 e^{\int \tilde{M}_{11} dN} \propto \frac{\delta\phi_1}{v} \quad (58)$$

is conserved. In inflation with two effective fields, the entropy mode $\delta\phi_2$ is unsourced, so the quantity

$$\delta\phi_2 e^{\int \tilde{M}_{22} dN} \quad (59)$$

is conserved. (Thus, in the special case of two-field inflation, the above expression for $\delta\phi_2$ can be plugged into Eq. (53) to find a semianalytic expression for $\delta\phi_1$, eliminating the need to solve a set of coupled equations [13].) Therefore, we make the important observation that *Eq. (57) is the multi-field generalization of the well-known single-field conservation equation for the adiabatic mode in Eq. (58)*. Eq. (57) endows each of the d modes with a conservation equation that holds whenever \mathbf{e}_n is not turning, $M_{n,n-1} = M_{n,n+1} = 0$, and $R_{nm} = 0$ for all $m \neq n$ (or when the sourcing terms in aggregate sum to zero). So there are up to d potential conserved quantities related to the modes.

Next, we consider how sourcing affects the evolution of the $\delta\phi_n$ mode. According to Eq. (55), sourcing effects can arise from:

1. Off-diagonal terms in the mass matrix
2. Any nontrivial geometry of the field manifold
3. The kinematical basis vectors changing direction

We will consider each sourcing effect in turn.

The first type of sourcing effect is a geometric effect that arises from off-diagonal terms in the covariant Hessian, \mathbf{M} , of the inflationary potential. Specifically, the mass matrix \mathbf{M} introduces terms of the form $-M_{n,n-1}\delta\phi_{n-1}$ and $-M_{n,n+1}\delta\phi_{n+1}$ into the sourcing equation for $\delta\phi_n$. These terms can be viewed as measures of the coupling between fields in the potential and of whether this coupling results in a higher or lower potential energy state. Or in the geometric picture, the terms $M_{n,n-1}$ and $M_{n,n+1}$ represent how much the n th component of the covariant derivative of $\ln V$ varies along

⁸ We caution the reader that the mode amplitude should not be assumed to decay approximately as $e^{-\tilde{M}_{nn}^* N_*}$, where \tilde{M}_{nn}^* is the value of the effective mass at horizon exit and N_* is the number of e-folds since the mode exited the horizon. As we discussed in [13] for the case of two-field inflation, this assumption often leads to large inaccuracies in estimating the mode amplitudes and the spectra. See [13] and references therein for further discussion of this issue.

⁹ However, we note that very often the curvature term is smaller than the mass M_{nn} , and so frequently, $\tilde{M}_{nn} \approx M_{nn}$.

the \mathbf{e}_{n-1} ($M_{n,n-1}$) and \mathbf{e}_{n+1} ($M_{n,n+1}$) directions. If the coupling term $M_{n,n+1}$ (or $M_{n,n-1}$) is positive, then $\delta\phi_{n+1}$ ($\delta\phi_{n-1}$) will cause $\delta\phi_n$ to decay; otherwise, if it is negative, it will increase the amplitude of $\delta\phi_n$. And the greater these geometric features in the potential, the stronger the sourcing effects will be. Interestingly, since the mass matrix is symmetric, a nonzero $M_{n,n+1}$ leads to parallel sourcing effects; for example, a negative value for $M_{n,n+1}$ will cause both the $\delta\phi_n$ and $\delta\phi_{n+1}$ modes to grow.¹⁰ Therefore, knowing either the mathematical form of the inflationary potential or the potential's geometric shape provides insight into the nature of the sourcing effects.

Likewise, the geometry of the field manifold can also cause sourcing effects. As explained earlier, the form of the kinetic terms in the inflationary Lagrangian can be represented through a field metric, and this metric can be viewed as inducing a field manifold. If the field manifold has nontrivial geometry, then the Riemann curvature tensor will be nonzero, and this will be manifested in the form of a nonzero symmetric curvature matrix $R_d^a \equiv 2\epsilon R_{bcd}^a e_1^b e_1^c$. Specifically, if the \mathbf{e}_m component of the failure of \mathbf{e}_1 to be parallel transported around the closed loop defined by \mathbf{e}_1 and \mathbf{e}_n is nonzero, then the curvature matrix will cause $\delta\phi_m$ to source $\delta\phi_n$. Since the curvature matrix can be factored into ϵ times a term involving the Riemann tensor, this term technically combines geometric and kinematical effects; so when all else is equal, the impact of noncanonical terms on the mode sourcing tends to be greatest at the end of inflation and whenever else the field speed is large. For this reason, the curvature matrix may be better viewed as a measure of the impact of nontrivial kinetic terms on the mode sourcing. However, for simplicity, we tend to refer to this type of sourcing effect as a geometrical effect arising from the field manifold. Now like the mass matrix, since the curvature matrix is symmetric, a positive value for a given curvature matrix coefficient will cause both the $\delta\phi_m$ and $\delta\phi_n$ modes to grow. However, in comparison to the sourcing effects due to the mass matrix coefficients, there are two key differences: (1) the curvature matrix can in principle couple together any two modes, and (2) the curvature matrix appears in the equation of motion with the opposite sign. Thus, we may view the mass matrix and curvature matrix as together encapsulating the sourcing effects due to the geometry of the Lagrangian, with the mass matrix primarily corresponding to the potential and the curvature matrix to the kinetic terms.

The third and last kind of sourcing effect is purely a kinematical effect—a direct consequence of the kinematical basis vectors changing direction. Consider the term $Z_{n+1,n}\delta\phi_{n+1}$ in Eq. (55). The kinematical term $Z_{n+1,n}$ represents how quickly the \mathbf{e}_n basis vector is turning into

Sourcing Terms	What the Terms Represent
$M_{n,n-1}, M_{n,n+1}$	Covariant Hessian of Potential (geometry of potential)
R_{nm}	Riemann Tensor of Field Manifold, ϵ (geometry of field manifold, kinematics)
$Z_{n,n-1}, Z_{n,n+1}$	Turn Rate of \mathbf{e}_n (kinematics)

TABLE I. The three types of sourcing effects in the mode sourcing equation for $\delta\phi_n$ and what each set of terms effectively represents. More detailed explanation of the terms and their impact on mode sourcing is given in the text below.

the direction of the \mathbf{e}_{n+1} basis vector. Since $Z_{n+1,n}$ is always non-negative, this turning will always cause $\delta\phi_n$ to grow. And the faster \mathbf{e}_n is turning into the \mathbf{e}_{n+1} direction, the more $\delta\phi_{n+1}$ sources $\delta\phi_n$. This sourcing effect can be interpreted physically as follows: the direct rotation of the kinematical basis vectors causes what was once a $\delta\phi_{n+1}$ mode to be partially converted into a $\delta\phi_n$ mode. The other kinematical sourcing term, $-Z_{n,n-1}\delta\phi_{n-1}$, can be understood similarly. However, this term causes $\delta\phi_n$ to shrink in magnitude, which can be explained by the fact that $\delta\phi_n$ is being partially converted into $\delta\phi_{n-1}$ by the rotation of basis vectors. The anti-symmetry of the turn rate matrix neatly encapsulates these antithetical kinematic effects.

A natural question that arises is whether the kinematical terms in the turn rate matrix represent some geometric feature of the Lagrangian. The answer is that while they can be expressed in terms of V and the field metric via Eq. (37), this expression is not geometrically transparent and does not boil down to a simple geometric feature. For example, one might expect that the mass matrix somehow effectively determines all the turn rates, but in general it does not, and the turn rates involve more complex combinations of the various n th-order covariant derivatives of $\ln V$. The only common exception occurs in the case of quadratic potentials with canonical kinetic terms (which is covered in Section III C 3), where it turns out that all the turn rates can indeed be expressed in terms of coefficients of the mass matrix. This leads to a very special simplification in the mode sourcing equations and also offers new insight into multi-field inflation. But in other scenarios, it is often easiest to view the effects from the turn rate matrix as kinematical effects, rather than particular geometric effects.

¹⁰ Again, when working in the classical picture, our statements are with respect to positive field fluctuations; it is straightforward to extrapolate to other cases.

2. Special Case I: Canonical kinetic terms

When the kinetic terms are canonical (or less stringently, when \mathbf{R} is no more complex than tridiagonal in the kinematical basis), the sourcing equations simplify further. In this common case, the mode sourcing equation for the adiabatic mode is unchanged in form. However, the slow-roll mode sourcing equations for the entropy modes simplify to

$$\delta\phi'_2 + \tilde{M}_{22}\delta\phi_2 \approx -(\tilde{M}_{23} - Z_{32})\delta\phi_3 \quad (60)$$

and

$$\begin{aligned} \delta\phi'_n + \tilde{M}_{nn}\delta\phi_n \approx & -(\tilde{M}_{n,n-1} + Z_{n,n-1})\delta\phi_{n-1} \\ & -(\tilde{M}_{n,n+1} - Z_{n+1,n})\delta\phi_{n+1}, \end{aligned} \quad (61)$$

for $n \geq 3$. Therefore, when the kinetic terms are canonical, only up to two modes, $\delta\phi_{n-1}$ and $\delta\phi_{n+1}$, can source the $\delta\phi_n$ mode in the slow-roll limit. Solving this series of coupled equations for the modes is tantamount to solving slow-roll Eq. (47) where the matrix sum $\tilde{\mathbf{M}} + \mathbf{Z}$ is tridiagonal.

3. Special Case II: Quadratic potentials with canonical kinetic terms

When the kinetic terms are canonical and the potential is quadratic—meaning that it satisfies

$$\nabla\nabla\nabla V = \mathbf{0} \quad (62)$$

—then the mode equations simplify even further. Since $\nabla^n V = \mathbf{0}$ for $n \geq 3$, it follows that $(\frac{D}{dN})^p \mathbf{M}$, where $p \geq 0$, is a function of only $\nabla \ln V$ and \mathbf{M} . Therefore, projecting the kinematical vectors in Eq. (50) onto the basis vectors yields

$$Z_{n+1,n} = \frac{\chi_{(n)}^{(n+1)}}{\chi_n^{(n)}} \approx -M_{n+1,n}. \quad (63)$$

That is, the mass matrix coefficient $-M_{n+1,n}$ gives the rate at which the \mathbf{e}_n basis vector turns into the direction of the \mathbf{e}_{n+1} basis vector. Substituting this result into Eq.

(61), the mode sourcing equation for all modes reduces to

$$\delta\phi'_n + M_{nn}\delta\phi_n \approx 2Z_{n+1,n}\delta\phi_{n+1}. \quad (64)$$

Therefore, for quadratic potentials with canonical kinetic terms, the $\delta\phi_n$ mode is sourced only by the $\delta\phi_{n+1}$ mode and only when the \mathbf{e}_n basis vector is covariantly changing direction into the \mathbf{e}_{n+1} direction. Mathematically, the solution for the n th mode is

$$\begin{aligned} \delta\phi_n \approx & \delta\phi_n^* e^{-\int_{N_*}^N M_{nn} dN_1} \\ & + \int_{N_*}^N 2Z_{n+1,n}\delta\phi_{n+1} e^{-\int_{N_*}^{N_1} M_{nn} dN_2} dN_1, \end{aligned} \quad (65)$$

where $*$ denotes a quantity is to be evaluated at horizon exit. In principle, one could solve the above series of integrals. Finally, since there is no sourcing when $Z_{n+1,n} = 0$, the number of kinematical basis vectors that are changing direction inversely indicates the number of conserved mode quantities.

4. Prescription for analyzing how Lagrangian differences affect mode sourcing

Taking a closer look at the special result in Eq. (63) for quadratic potentials, this result follows from the more general result in Eq. (50) that

$$Z_{n+1,n} \approx -M_{n+1,n} + \text{corrections}. \quad (66)$$

These so-called “corrections” depend on certain projections of the higher-order covariant derivatives of $\ln V$; that is, each term contains at least one quantity $\nabla^p V$, where $p \geq 3$. The highest-order term in the series of corrections involves $\nabla^n V$, and the sum of correction terms truncates prematurely if $\nabla^p V$ vanishes for all p greater than some positive integer but less than n . Interestingly, plugging Eq. (66) into the general mode sourcing equation (55) tells us that the sourcing of $\delta\phi_n$ by $\delta\phi_{n-1}$ is controlled by these certain projections of the higher-order covariant derivatives $\nabla^p \ln V$, where $p \geq 3$. Similarly, we can view the sourcing of $\delta\phi_n$ by $\delta\phi_{n+1}$ to be controlled by a term that is twice the turn rate $Z_{n+1,n}$, plus corrections from higher-order covariant derivatives of $\ln V$. And of course, any nonzero R_{mn} terms arising from noncanonical kinetic terms would contribute additional sourcing effects. In other words, we can view the entropy mode sourcing equations as

$$\begin{aligned} \delta\phi'_n + \tilde{M}_{nn}\delta\phi_n \approx & -(\text{corrections from potential})\delta\phi_{n-1} + (2Z_{n+1,n} + \text{corrections from potential})\delta\phi_{n+1} \\ & + \frac{1}{3} \sum_{m=2, m \neq n}^d R_{nm}\delta\phi_m, \end{aligned} \quad (67)$$

where the “corrections” are certain projections of the covariant higher-order derivatives of the potential, as explained above. This results in a very interesting and useful way to view the interactions among modes: *the interactions can essentially be divided into sourcing effects shared in common with canonical quadratic models ($Z_{n+1,n}$ terms) and sourcing effects arising from deviations from this fundamental Lagrangian (the “corrections” and R_{nm} terms).* We advocate this novel approach as a powerful prescription for exploring how differences in Lagrangians translate into differences in mode dynamics.

This completes our more rigorous and physically-motivated study of the interactions among modes in general multi-field inflation.

IV. EFFECTIVE NUMBER OF FIELDS AND THE SPECTRAL OBSERVABLES

In Sections II and III, we explored how the inflationary geometry and kinematics affect the evolution of modes. In this section, we discuss how this in turn translates into the cosmic observables. But since determining how the geometry and kinematics affects the mode interactions is most of the battle, we will not rehash any connections that can easily be inferred from our discussion in Section III C. Instead, here we will focus more on how the inflationary geometry and kinematics determine the effective number of inflationary fields and how this is reflected in the cosmic power spectra, bispectrum, and trispectrum. We start in Section IV A by discussing how the kinematics and geometry of inflation determine the effective number of fields. In Sections IV B-IV D, we discuss the multi-field results for the power spectra, bispectrum, and trispectrum. In the process of doing so, we introduce a new cosmic *multi-field observable* that distinguishes two-field models from models with three or more fields, and we present a new multi-field consistency relation.

A. Effective Number of Fields

Having laid the groundwork for determining the sourcing relationships among the modes, we can now consider the effective number of fields in a multi-field scenario. We define the effective number of fields to be the minimum number of fields necessary to adequately describe an inflationary potential and reproduce the results for the cosmic observables across the distance scales of interest. The effective number of fields can also be thought of as the *dimension* of inflation.

We start by considering the minimum number of fields required to produce a given background solution. In order to adequately describe the background solution, we must have enough fields to reproduce all the kinematical vectors, as defined in Eq. (14). That is, we must have enough kinematical basis vectors to span the space defined by the kinematical vectors, and the minimum

number of these basis vectors gives the dimension of the background solution. Because of the way we constructed the kinematical basis vectors in Eq. (16), the dimension also equals one plus the number of kinematical basis vectors that are changing direction. In particular, if the \mathbf{e}_1 basis vector is changing direction, then the inflationary scenario has at least two effective field degrees of freedom. Of course, at a given moment, the effective field degrees of freedom may be fewer or greater than it is at other times. To determine an effective dimension for an entire multi-field scenario, one can simply take the maximum dimension of the kinematical vectors that exists between the start of that scenario until the end of inflation. This is illustrated in Figure 1. In scenarios with canonical kinetic terms that are effectively described by one field, the trajectory in field space will resemble a line. Similarly, the trajectories of scenarios with two effective fields will reside in a plane.

The effective dimension of the field perturbations, however, is more complicated to determine. We define the effective dimension of the modes as the minimum number of independent field perturbations we must consider in order to calculate the spectra. Based on the spectra we consider, this is equivalent to the number of fields we must consider in order to find solutions for $\delta\phi_1$ and $\delta\phi_2$; why this is so will become clearer in the next two sections.

Consider first the particular case where the \mathbf{e}_1 basis vector never turns. In this case, the adiabatic mode is never sourced and the quantity $\frac{\delta\phi_1}{v}$ is conserved in the superhorizon limit. While the effective dimension of the unperturbed fields is one, the dimension of the perturbed fields can be either one or more: it is one if there is only one field and hence there are no entropy modes, but it is more if there are two or more fields during inflation and hence a power spectrum of entropy modes.

In the case where the field trajectory does change direction during inflation, there are two reasons why the effective dimension of the background and perturbed fields do not necessarily coincide. The first reason is that the curvature matrix \mathbf{R} can couple together the various entropy modes, independently of the turning behavior of the kinematical basis vectors. Second, in general, it is not true that $M_{n+1,n} \approx -Z_{n,n+1}$. So even if the kinematical basis vectors are not turning, a nonzero $M_{n+1,n}$ could still allow the $\delta\phi_{n+1}$ mode to source the $\delta\phi_n$ mode. (Of course, for many models, when $Z_{n+1,n} = 0$, it will also be true that $M_{n+1,n} = 0$.) Therefore, for models with at least two fields, the effective number of field perturbations we need to consider in order to find expressions for $\delta\phi_1$ and $\delta\phi_2$ will equal two plus the number of consecutive nonzero terms $\tilde{M}_{n+1,n} + Z_{n+1,n}$ when we count upwards starting from $n = 2$. This follows directly from the series of slow-roll sourcing equations in Eq. (55). Based on this analysis, we take the effective dimension of the perturbed field system, which can be larger than the dimension of the unperturbed system, as the overall effective dimension of a multi-field scenario.

Yet, although we can assign an overall dimension to each scenario, it is also useful to consider that an inflationary scenario may be broken into multiple phases, with each one defined by a different effective number of fields being active. For example, in canonical quadratic models with very different masses for the fields in the potential, there are periods dominated by the dynamics of a single-field, punctuated by periods in which two fields dominate the dynamics. By understanding that a model with multiple fields can be approximated by a series of scenarios with a much smaller effective dimension—in the example, a series of single-field and two-field scenarios—we can gain much greater insight into the key features of such models, and they become much more computationally tractable.

B. Tensor and Curvature Power Spectra

With this newfound understanding, we explore the main spectral observables to see how they reflect the effective dimension and the main features of multi-field scenarios. We tackle these observables in rather quick succession, so we refer the interested reader to [13, 17, 21, 23, 30] for more details about how these quantities are calculated.

We start with the power spectra. The tensor power spectrum is unchanged by the presence of multiple fields and has the form [67]

$$P_T = 8 \left(\frac{H_*}{2\pi} \right)^2, \quad (68)$$

under the common convention for normalization of the spectrum.

The density power spectrum is typically given in terms of the power spectrum of curvature perturbations, as the two are equivalent up to factors of $O(1)$ after inflation ends. The curvature perturbation \mathcal{R} during inflation is related to the adiabatic density mode by [19]

$$\mathcal{R} = \frac{\delta\phi_1}{v}. \quad (69)$$

Using the mode sourcing equation for the adiabatic mode and quantizing the fields, one can find the curvature

power spectrum. Using the notation in this paper, the curvature power spectrum at the end of inflation [23] can be rewritten as

$$\mathcal{P}_{\mathcal{R}} = \left(\frac{H_*}{2\pi} \right)^2 \frac{1}{2\epsilon_*} \left(1 + |\mathbf{T}_{\mathcal{RS}}|^2 \right), \quad (70)$$

where it is understood that the function $\mathbf{T}_{\mathcal{RS}}$ is evaluated at the end of inflation and where

$$\begin{aligned} \mathbf{T}_{\mathcal{RS}}(N) &\equiv \int_{N_*}^N 2 \left| \frac{D\mathbf{e}_1}{dN} \right| \mathbf{T}_{\mathcal{SS}}(N_1) dN_1, \\ \mathbf{T}_{\mathcal{SS}}(N) &\equiv \frac{\mathbf{e}_2^\dagger}{v} e^{-\int_{N_*}^N (\tilde{\mathbf{M}}_{\perp\perp} + \mathbf{Z}_{\perp\perp}) dN_1}, \end{aligned} \quad (71)$$

to lowest order in the slow-roll limit. We also made the replacement $\tilde{\mathbf{M}} + \mathbf{Z} \rightarrow \tilde{\mathbf{M}}_{\perp\perp} + \mathbf{Z}_{\perp\perp}$, which follows from the fact that the $\delta\phi_2$ entropy mode can only be sourced by the other entropy modes.

Examining Eq. (70), the curvature spectrum at the end of inflation equals the curvature spectrum at horizon exit plus corrections dictated by the function $\mathbf{T}_{\mathcal{RS}}$.¹¹ The function $\mathbf{T}_{\mathcal{SS}}$ represents the evolution of the entropy-mode-related quantity $\frac{\delta\phi_2}{v}$, taking into account both the mode's intrinsic evolution and the effects of entropy mode sourcing. The other function, $\mathbf{T}_{\mathcal{RS}}$, is a measure of how much $\frac{\delta\phi_2}{v}$ sources the curvature mode—or more liberally speaking, of how much $\delta\phi_2$ sources $\delta\phi_1$. The forms of the transfer functions follow directly from Eqs. (48) and (52). We call $\mathbf{T}_{\mathcal{RS}}$ and $\mathbf{T}_{\mathcal{SS}}$ the *multi-field transfer functions* or simply the *transfer functions* since they are the multi-field generalization of the scalar transfer functions in two-field inflation [33, 66]. The difference is that there are multiple entropy modes in general multi-field inflation, so the transfer functions are necessarily vectors rather than scalar functions.

Looking at $\mathbf{T}_{\mathcal{SS}}$ more closely, it involves the exponential of the integral of a matrix, which can be estimated using the Magnus series expansion. According to the Magnus series expansion (see [68] and references therein), if we take $e^{\mathbf{\Omega}(N)} \equiv e^{-\int_{N_*}^N (\tilde{\mathbf{M}}_{\perp\perp} + \mathbf{Z}_{\perp\perp}) dN_1}$, then the first three terms in the series expansion are

¹¹ We use the symbol $\mathbf{T}_{\mathcal{RS}}$ rather than Nibbelink and van Tent's symbol \mathbf{U}_{P_e} in order to mirror the transfer function notation

used for two-field inflation [13, 33, 66].

$$\begin{aligned}
\Omega_1 &= - \int_{N_*}^N (\tilde{\mathbf{M}} + \mathbf{Z})_{\perp\perp} dN_1, \\
\Omega_2 &= \frac{1}{2} \int_{N_*}^N \int_{N_*}^{N_1} [(\tilde{\mathbf{M}} + \mathbf{Z})_{\perp\perp}(N_1), (\tilde{\mathbf{M}} + \mathbf{Z})_{\perp\perp}(N_2)] dN_2 dN_1, \\
\Omega_3 &= - \frac{1}{3!} \int_{N_*}^N \int_{N_*}^{N_1} \int_{N_*}^{N_2} ([(\tilde{\mathbf{M}} + \mathbf{Z})_{\perp\perp}(N_1), [(\tilde{\mathbf{M}} + \mathbf{Z})_{\perp\perp}(N_2), (\tilde{\mathbf{M}} + \mathbf{Z})_{\perp\perp}(N_3)]) \\
&\quad + [(\tilde{\mathbf{M}} + \mathbf{Z})_{\perp\perp}(N_3), [(\tilde{\mathbf{M}} + \mathbf{Z})_{\perp\perp}(N_2), (\tilde{\mathbf{M}} + \mathbf{Z})_{\perp\perp}(N_1)]] dN_3 dN_2 dN_1,
\end{aligned} \tag{72}$$

where $[\mathbf{A}, \mathbf{B}] \equiv \mathbf{AB} - \mathbf{BA}$ is the matrix commutator of matrices \mathbf{A} and \mathbf{B} . Note that because $\tilde{\mathbf{M}}$ and \mathbf{Z} are symmetric and anti-symmetric, respectively, the commutator $[\tilde{\mathbf{M}}, \mathbf{Z}] = 0$, and hence the above expressions further simplify, with the result being only commutators of each matrix with itself at different time points remain. The computational complexity of the Magnus series expansion vividly illustrates how advantageous it is to use simplifications. For every mode degree of freedom that we can ignore, the calculation of the matrix exponential greatly simplifies. Hence we strongly emphasize the importance of using our newfound result that \mathbf{M} is a tridiagonal symmetric matrix in the slow-roll limit in the kinematical basis, of determining the effective dimension of a multi-field scenario, and of exploiting matrix symmetry and anti-symmetry properties to simplify the commutators.

Now the geometry and kinematics of the inflationary Lagrangian affect the curvature spectrum through the quantities H_* , $2\epsilon_*$, and $\mathbf{T}_{\mathcal{RS}}$ (which in turn depends on $\mathbf{T}_{\mathcal{SS}}$). The quantities H_* and ϵ_* straightforwardly depend on the Lagrangian geometry since they are functions of V_* and $|\nabla_* \ln V|$, respectively. The third quantity is more complicated. It depends on the turn rate of the background trajectory times the transfer function $\mathbf{T}_{\mathcal{SS}}$, a vector function representing how much the $\delta\phi_2$ mode itself is sourced by the other $d-1$ entropy modes. But fortunately, the behavior of $\mathbf{T}_{\mathcal{RS}}$ can be inferred from our classical treatment of the mode sourcing equations. For example, if the \mathbf{e}_2 basis vector is rapidly turning into the \mathbf{e}_3 direction while \mathbf{e}_1 turns at a constant rate, then $\delta\phi_2$ will be strongly sourced by $\delta\phi_3$, causing a boost in the amplitude of both transfer functions. As a second example, if the field trajectory rolls along and parallel to a ridge in the potential, then the $\delta\phi_2$ mode will grow in amplitude, causing a boost in $\mathbf{T}_{\mathcal{SS}}$ and a greater than perhaps expected boost in $\mathbf{T}_{\mathcal{RS}}$. As a third example, if a strong negative curvature R_{32} arises from the kinetic terms in the Lagrangian and dominates the dynamics of the $\delta\phi_2$ and $\delta\phi_3$ modes, both modes will decay, thereby reducing $\mathbf{T}_{\mathcal{SS}}$ and blunting the sourcing function $\mathbf{T}_{\mathcal{RS}}$. This demonstrates that the effects of the geometry and kinematics of the Lagrangian on the curvature spectrum follow directly from all the connections we made in Sec-

tion III C between the mode sourcing and the geometry and kinematics of inflation. Thus, we emphasize that one can understand how the Lagrangian translates into cosmic observables by studying the mode sourcing in detail.

Next, to determine how the effective number of fields is reflected in the curvature spectrum, we define a new unit vector

$$\mathbf{e}_{\mathcal{R}} \equiv \frac{\mathbf{T}_{\mathcal{RS}}}{|\mathbf{T}_{\mathcal{RS}}|} \tag{73}$$

and the scalar quantity

$$T_{\mathcal{RS}} \equiv |\mathbf{T}_{\mathcal{RS}}|. \tag{74}$$

The unit vector $\mathbf{e}_{\mathcal{R}}$ necessarily lies in the $(d-1)$ -dimensional subspace spanned by the kinematical basis vectors $\mathbf{e}_2^*, \mathbf{e}_3^*, \dots, \mathbf{e}_d^*$, where again $*$ represents that a quantity is evaluated at horizon exit. If inflation has two effective fields, then $\mathbf{e}_{\mathcal{R}} = \mathbf{e}_2^*$; however, if inflation has more than two effective fields, then $\mathbf{e}_{\mathcal{R}} \neq \mathbf{e}_2^*$. Moreover, one plus the number of nonzero components of $\mathbf{e}_{\mathcal{R}}$ in the kinematical basis gives the effective number of fields. We use the above quantities to rewrite the power spectrum for general multi-field inflation as

$$\mathcal{P}_{\mathcal{R}} = \left(\frac{H_*}{2\pi}\right)^2 \frac{1}{2\epsilon_*} (1 + T_{\mathcal{RS}}^2). \tag{75}$$

Recall that in single-field inflation, $T_{\mathcal{RS}} = 0$, and the single-field curvature power spectrum is $\frac{1}{16\epsilon_*}$ times larger than the tensor spectrum. That is, the tensor-to-scalar ratio r_T , defined by

$$r_T \equiv \frac{\mathcal{P}_{\mathcal{R}}}{\mathcal{P}_T}, \tag{76}$$

produces the single-field consistency relation

$$r_T = -8n_T, \tag{77}$$

where the tensor spectral index $n_T \equiv \frac{d \ln \mathcal{P}_T}{d \ln k} \approx -2\epsilon_*$. In multi-field inflation, however, the ratio satisfies the upper bound [13, 33]:

$$r_T = -8n_T \cos^2 \Delta_N \leq -8n_T, \tag{78}$$

where

$$\tan \Delta_N = T_{\mathcal{R}\mathcal{S}}. \quad (79)$$

But beyond this, the curvature power spectrum cannot provide any further clues about the effective number of fields during multi-field inflation. The reason why is because Eq. (75) is identical in form to the corresponding expression for two-field inflation [13]. To probe the number of effective fields during inflation, we have to obtain information on the number of non-zero components of $\mathbf{e}_{\mathcal{R}}$, which is not possible to do with only the tensor and curvature power spectra.

As an aside, the multi-field curvature power spectrum can also be given in terms of the δN formalism. Under the δN formalism, correlators of \mathcal{R} can be written in terms of covariant derivatives of N , so the curvature power spectrum can be written as [17]

$$\mathcal{P}_{\mathcal{R}} = \left(\frac{H_*}{2\pi} \right)^2 |\nabla N|^2, \quad (80)$$

where ∇N is the covariant derivative of the number of e-folds of inflation. By comparing Eqs. (70) and (80) and using that $\mathbf{e}_1^* \cdot \mathbf{e}_{\mathcal{R}} = 0$, it follows that

$$\nabla^\dagger N = \frac{1}{\sqrt{2\epsilon_*}} (\mathbf{e}_1^* + T_{\mathcal{R}\mathcal{S}} \mathbf{e}_{\mathcal{R}}), \quad (81)$$

and therefore, the unit vector in the direction of $\nabla^\dagger N$ is

$$\mathbf{e}_N = \cos \Delta_N \mathbf{e}_1^* + \sin \Delta_N \mathbf{e}_{\mathcal{R}}. \quad (82)$$

These results generalize those found for two-field inflation in [69] and will be useful later when we calculate the non-Gaussianity arising from multi-field inflation.

C. Isocurvature and Cross Spectra

If there is more than one field present, then there will also be a relic spectrum of entropy modes and a cross spectrum between the density and entropy modes. Therefore, the detection of an entropy mode spectrum arising from inflation would indicate that inflation is multi-field. In lieu of the entropy modes, one usually works in terms of isocurvature modes \mathcal{S} , which can be defined in a gauge-invariant and dimensionless manner:

$$\mathcal{S} \equiv \frac{\delta p}{p'} - \frac{\delta \rho}{\rho'}. \quad (83)$$

Up to normalization factors, it can be shown that \mathcal{S} depends on only the entropy mode $\delta\phi_2$. Here, we choose the normalization factor so that the isocurvature and curvature spectra have equal power at horizon crossing:

$$\mathcal{S} \equiv \frac{\delta\phi_2}{v}. \quad (84)$$

Under these above assumptions and using some prior results from [13, 23], the isocurvature spectrum at the end of inflation is

$$\mathcal{P}_{\mathcal{S}} = \left(\frac{H_*}{2\pi} \right)^2 \frac{1}{2\epsilon_*} |\mathbf{T}_{\mathcal{S}\mathcal{S}}|^2, \quad (85)$$

where $\mathbf{T}_{\mathcal{S}\mathcal{S}}$ is given by Eq. (71) and is calculated at the end of inflation.

Now, unlike for the curvature modes, determining the isocurvature spectrum in the period after inflation ends is much more complicated. After inflation ends, the isocurvature modes may decay further, affecting the amplitude of the isocurvature spectrum at the time of the CMB. But such post-inflationary processing is highly model dependent and depends on the dynamics of reheating, among other factors. So to keep our discussion as simple and as broadly applicable as possible, we focus only on the amplitude of the isocurvature modes at the end of inflation. Any post-inflationary modification of the isocurvature modes can always be tacked onto these results, and so these results can be construed as upper limits on the amplitude of isocurvature modes.

Like in the previous section, how the geometry and kinematics of inflation affects the spectrum follows from our detailed discussion of the mode sourcing in Section III C. So let us proceed by considering how the number of fields is reflected in the isocurvature spectrum. Like for the other transfer function, we can break $\mathbf{T}_{\mathcal{S}\mathcal{S}}$ into two parts:

$$\begin{aligned} \mathbf{e}_{\mathcal{S}} &\equiv \frac{\mathbf{T}_{\mathcal{S}\mathcal{S}}}{|\mathbf{T}_{\mathcal{S}\mathcal{S}}|}, \\ T_{\mathcal{S}\mathcal{S}} &\equiv |\mathbf{T}_{\mathcal{S}\mathcal{S}}|. \end{aligned} \quad (86)$$

In the case of two-field inflation, $\mathbf{e}_{\mathcal{S}} = \mathbf{e}_2^*$, whereas for inflation with three or more effective fields, $\mathbf{e}_{\mathcal{S}} \neq \mathbf{e}_2^*$. Using these two quantities, the multi-field isocurvature spectrum is

$$\mathcal{P}_{\mathcal{S}} = \left(\frac{H_*}{2\pi} \right)^2 \frac{1}{2\epsilon_*} T_{\mathcal{S}\mathcal{S}}^2. \quad (87)$$

Like for the curvature spectrum, the expression for the multi-field isocurvature spectrum has the same form as in the two-field case and therefore does not provide us any insight into the number of fields present during inflation, at least not to lowest-order in the slow-roll expansion.

Also if inflation is multi-field, there will be a cross spectrum between the curvature and isocurvature modes, representing the correlations between the two modes. Again combining results from [13, 23], we write the cross spectrum as

$$\mathcal{C}_{\mathcal{R}\mathcal{S}} = \left(\frac{H_*}{2\pi} \right)^2 \frac{1}{2\epsilon_*} (\mathbf{T}_{\mathcal{R}\mathcal{S}} \cdot \mathbf{T}_{\mathcal{S}\mathcal{S}}). \quad (88)$$

Obviously, inflation is necessarily single-field if there is no cross spectrum, but let us consider if the cross-spectrum can provide any information into the number

of fields during multi-field inflation. Using Eqs. (73) and (86), the cross-spectrum can be written as

$$\mathcal{C}_{\mathcal{RS}} = \left(\frac{H_*}{2\pi} \right)^2 \frac{1}{2\epsilon_*} T_{\mathcal{RS}} T_{SS} (\mathbf{e}_{\mathcal{R}} \cdot \mathbf{e}_{\mathcal{S}}). \quad (89)$$

Now comparing the above result to [13], we see that the above result is identical to the two-field result with the exception of the term $\mathbf{e}_{\mathcal{R}} \cdot \mathbf{e}_{\mathcal{S}}$. This is the first instance of a spectral quantity whose expression differs from the two-field case and hence can potentially be used to gain more insight into the effective dimension of a multi-field system. If $\mathbf{e}_{\mathcal{R}} \cdot \mathbf{e}_{\mathcal{S}} = 1$, as is automatically true for two-field inflation, then we recover the two-field result. However, if the two unit vectors are not parallel to each other, then there must be three or more fields present during inflation, and this should be reflected in the cross spectrum. We can therefore use the cross spectrum to devise a test that will distinguish inflation with three or more fields from inflation with two fields. In analogy to the tensor-to-scalar ratio, we define the cross-correlation ratio as [32]

$$r_C \equiv \frac{\mathcal{C}_{\mathcal{RS}}}{\sqrt{\mathcal{P}_{\mathcal{R}} \mathcal{P}_{\mathcal{S}}}}, \quad (90)$$

which implies that

$$r_C = \sin \Delta_N \mathbf{e}_{\mathcal{R}} \cdot \mathbf{e}_{\mathcal{S}}. \quad (91)$$

Substituting Eq. (97) into Eq. (91), we obtain

$$r_C \leq \sqrt{1 + \frac{r_T}{8n_T}}, \quad (92)$$

where equality implies the presence of only two effective fields and inequality implies three or more fields.

Based on these observations, it is therefore helpful to define two *multi-field parameters*

$$\begin{aligned} \beta_1 &\equiv \sqrt{-\frac{r_T}{8n_T}}, \\ \beta_2 &\equiv \frac{r_C}{\sqrt{1 + \frac{r_T}{8n_T}}}. \end{aligned} \quad (93)$$

The multi-field parameter β_1 distinguishes single-field inflation from multi-field inflation. It derives from the well-known single-field consistency relation in Eq. (77). When $\beta_1 = 1$, inflation is single-field; whereas, for multi-field inflation, $0 \leq \beta_1 \leq 1$. The second multi-field parameter β_2 distinguishes among multi-field models, differentiating two-field models from models with three or more fields. When $\beta_2 = 1$, inflation is driven by two fields, whereas for models with three or more fields, $0 \leq \beta_2 \leq 1$. Since we are not accounting for any possible post-inflationary decay of the isocurvature modes, in practice, β_2 is more informative when it equals 1 (signaling two fields), rather than when it is less than 1 (signaling either more than two fields or post-inflationary decay of the isocurvature modes). These results are summarized in Fig. 3.

Multi-Field Observables	
$\beta_1 \equiv \sqrt{-\frac{r_T}{8n_T}}$	$\beta_2 \equiv \frac{r_C}{\sqrt{1-\beta_1^2}}$

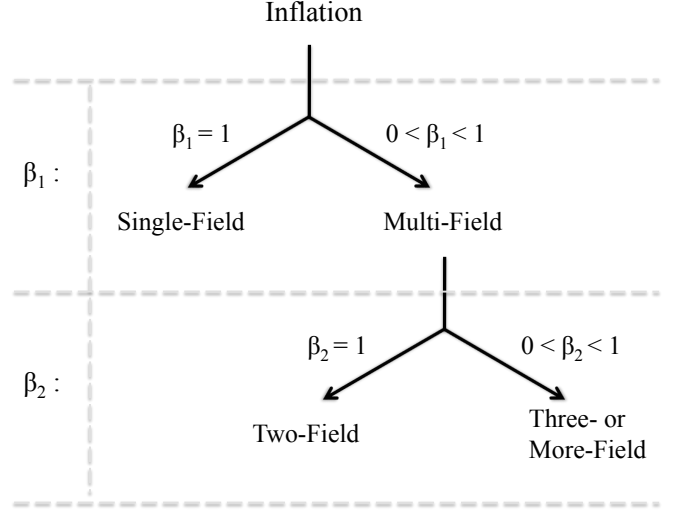


FIG. 3. Multi-field observables β_1 and β_2 indicate the effective number of fields during inflation.

In sum, the tensor, curvature, isocurvature, and cross-spectra can in principle be used to distinguish among inflationary models driven by one, two, and three or more fields. However, the caveat is that all four spectra must be measured.

D. Higher-Order Spectra

Let us consider whether other spectral observables provide any clues about the number of fields present during inflation. Another group of important cosmic observables are the Fourier transforms of higher-order mode correlation functions. These higher-order spectra represent the non-Gaussian behavior of the perturbations. The two lowest-order correlation functions are known as the bispectrum and trispectrum, respectively. For standard multi-field inflation, the local form of these curvature spectra predominate,¹² with the local bispectrum represented by the parameter f_{NL} and the trispectrum by the parameters τ_{NL} and g_{NL} . Using the δN formalism, the non-Gaussianity parameters can be expressed as [71–73]

¹² However, when $\mathbf{R} \neq \mathbf{0}$, other forms of the bispectra and trispectra may also be important. We only give the local form here.

$$\begin{aligned}
-\frac{6}{5}f_{NL} &= \frac{\mathbf{e}_N^\dagger \nabla^\dagger \nabla N \mathbf{e}_N}{|\nabla N|^2}, \\
\tau_{NL} &= \frac{\mathbf{e}_N^\dagger \nabla^\dagger \nabla N \nabla^\dagger \nabla N \mathbf{e}_N}{|\nabla N|^4}, \\
\frac{54}{25}g_{NL} &= \frac{\mathbf{e}_N^\dagger \nabla^\dagger \nabla \nabla N \mathbf{e}_N \mathbf{e}_N}{|\nabla N|^3}.
\end{aligned} \tag{94}$$

$$-\frac{6}{5}f_{NL} = \frac{1}{2} \cos^2 \Delta_N (n_{\mathcal{R}} - n_T) + \sin \Delta_N \cos \Delta_N \left[(\mathbf{e}_{\mathcal{R}}^\dagger M \mathbf{e}_1)^* + \sin \Delta_N \cos \Delta_N \sqrt{-n_T} \mathbf{e}_{\mathcal{R}} \cdot \nabla T_{\mathcal{RS}} \right]. \tag{95}$$

The only difference between the above result and the result for two-field inflation is that \mathbf{e}_2 has been replaced by $\mathbf{e}_{\mathcal{R}}$.

To find the trispectrum parameters, we also follow a similar procedure to [69]. For τ_{NL} , we obtain

$$\begin{aligned}
\tau_{NL} &= \frac{1}{\sin^2 \Delta_N} \left[\frac{6}{5}f_{NL} + \frac{1}{2} \cos^2 \Delta_N (n_{\mathcal{R}} - n_T) \right]^2 \\
&\quad + \frac{1}{4} \cos^2 \Delta_N (n_{\mathcal{R}} - n_T)^2.
\end{aligned} \tag{96}$$

Since

$$-\frac{r_T}{8n_T} = \cos^2 \Delta_N, \tag{97}$$

we can write τ_{NL} completely in terms of other spectral observables, which gives us a new consistency condition for general multi-field inflation:

$$\begin{aligned}
\tau_{NL} &= \frac{1}{1 + \frac{r_T}{8n_T}} \left[\frac{6}{5}f_{NL} - \frac{1}{2} \frac{r_T}{8n_T} (n_{\mathcal{R}} - n_T) \right]^2 \\
&\quad - \frac{1}{4} \frac{r_T}{8n_T} (n_{\mathcal{R}} - n_T)^2,
\end{aligned} \tag{98}$$

which is only valid when inflation contains multiple fields. In the limit where f_{NL} is detectably large (i.e., $|f_{NL}| \gtrsim 3$), the above multi-field consistency condition reduces to

$$\tau_{NL} \approx \frac{1}{1 + \frac{r_T}{8n_T}} \left(\frac{6}{5}f_{NL} \right)^2. \tag{99}$$

In this limit, the value of τ_{NL} relative to f_{NL}^2 is controlled solely by the ratio of r_T to n_T ; the larger the sourcing of the curvature mode by the isocurvature modes, the more τ_{NL} approaches $(\frac{6}{5}f_{NL})^2$. In other words, only multi-field inflationary scenarios where the multi-field effects are very weak can produce $\tau_{NL} \gg f_{NL}^2$.

Lastly, for the trispectrum parameter g_{NL} , we find

$$\begin{aligned}
\frac{54}{25}g_{NL} &= -2\tau_{NL} + 4 \left(\frac{6}{5}f_{NL} \right)^2 \\
&\quad + \sqrt{\frac{r_T}{8}} \mathbf{e}_N \cdot \nabla \left(-\frac{6}{5}f_{NL} \right).
\end{aligned} \tag{100}$$

In [69], we calculated the above non-Gaussianity parameters for two-field inflation by operating ∇ on the transfer function expression for $\nabla^\dagger N$ in Eq. (81). The calculation is similar for the case of general multi-field inflation. Repeating the steps we followed in [69], we obtain a semi-analytic formula for the bispectrum parameter:

As written, the above result for multi-field inflation is identical in form to that in two-field inflation.

Let us consider how the results for the three parameters f_{NL} , τ_{NL} , and g_{NL} reflect the effective number of fields. In single-field inflation, the expressions for the three parameters simplify nicely. In fact, the parameters f_{NL} [70], τ_{NL} [74], and g_{NL} each give rise to a single-field consistency relation:

$$\begin{aligned}
-\frac{6}{5}f_{NL} &= \frac{1}{2}(n_{\mathcal{R}} - n_T), \\
\tau_{NL} &= \left(\frac{6}{5}f_{NL} \right)^2, \\
\frac{54}{25}g_{NL} &= 2 \left(\frac{6}{5}f_{NL} \right)^2 + \left(-\frac{6}{5}f_{NL} \right)',
\end{aligned} \tag{101}$$

where $\frac{df_{NL}}{d \ln k} \approx f'_{NL}$ represents the scale dependence of f_{NL} and where we combined the single-field limits of Eq. (96) to obtain the last relation. Hence, a measurement of any one of the three non-Gaussian parameters can tell us whether inflation is single-field or multi-field. However, these parameters provide no additional insight into the effective number of fields present during multi-field inflation. The reason why is that their expressions in multi-field inflation are identical to those in two-field inflation after the replacement $\mathbf{e}_2^* \rightarrow \mathbf{e}_{\mathcal{R}}$, and hence they cannot differentiate models with two fields from those with three or more fields.

V. CONCLUSIONS

In this paper, we explored how the geometric and kinematical features of multi-field inflationary Lagrangians with noncanonical kinetic terms are reflected in the cosmic observables. We focused on how these geometric and kinematical features affect the interactions among modes and how this determines the effective number of active fields during inflation.

We started by presenting the covariant background equation of motion for the fields and by delineating a

framework to parse the kinematics of the background fields. The kinematics of the background fields induce a basis called the kinematical basis and a matrix of turn rates, \mathbf{Z} , which characterizes how quickly these basis vectors are rotating. This framework is important because working in the kinematical basis yields several advantages in elucidating the behavior of both the unperturbed and perturbed fields. We concluded our treatment of the background fields by discussing the slow-roll limit and certain subcases of limiting behavior.

Next, we explored the equation of motion for the field perturbations in both the given and kinematical bases. In the combined superhorizon and slow-roll limits, the equation of motion for the field perturbations depends only on the effective mass matrix $\tilde{\mathbf{M}}$ (a primarily geometrical tensor representing the covariant Hessian of the potential and the Riemann tensor of the field manifold) and the turn rate matrix \mathbf{Z} (a kinematical tensor). We then studied the mode interactions one by one, filling an important gap in the literature. To do so, we first proved that most of the coefficients of the mass matrix $\mathbf{M} \equiv \nabla^\dagger \nabla \ln V$ vanish in the kinematical basis. We used this result to derive a series of simplified mode sourcing equations for all the modes in the slow-roll limit. In particular, we found that for Lagrangians with canonical kinetic terms, the matrix sum $\mathbf{M} + \mathbf{Z}$ is tridiagonal in the kinematical basis, so the $\delta\phi_n$ entropy mode can only be sourced by the $\delta\phi_{n-1}$ and $\delta\phi_{n+1}$ entropy modes. For quadratic potentials with canonical kinetic terms, the equations simplify even further, in a way such that each mode $\delta\phi_n$ can be sourced only by $\delta\phi_{n+1}$ but only when the basis vector \mathbf{e}_n is turning into the direction of \mathbf{e}_{n+1} . We therefore argued that the mode interactions in a general inflation model can be divided into features shared in common with canonical quadratic models and features that arise from differences from this fundamental Lagrangian, and we advocated this approach as way to gain greater insight into how differences in Lagrangians translate into differences in the cosmic observables.

In parallel, we discussed how the geometric and kinematical features of multi-field inflationary Lagrangians affect the mode sourcing. We started by considering the case where the $\delta\phi_n$ mode is unsourced, and we discussed how the concavity of the potential and the curvature of the field manifold determine that mode's intrinsic evolution rate. We showed that there are up to d mode-related quantities in inflation with d scalar fields that may be conserved, thereby generalizing the single-field conservation law for the adiabatic mode. Next, we discussed how the sourcing effects for the $\delta\phi_n$ mode depend two types of geometrical terms and one type of kinematical term. The geometrical terms involve off-diagonal terms in both the covariant Hessian of the potential and in the Riemann tensor of the field metric contracted with two instances of \mathbf{e}_1 and modulated by ϵ , and we interpreted these terms geometrically. The kinematical terms are simply the turn rates of \mathbf{e}_n into the \mathbf{e}_{n-1} and \mathbf{e}_{n+1} directions. Although the turn rates can be expressed in terms of geometri-

cal features of the Lagrangian, these expressions are in general complicated and opaque, so it is usually easier to treat these terms as kinematical quantities. We also gave several examples of how inferences about the mode sourcing can be made by determining the geometric and kinematical features of a Lagrangian.

Determining how these geometric and kinematical features are reflected in the cosmic observables mostly boils down to understanding how the modes interact in the classical picture. Therefore, it is essential to study the interactions among modes as we demonstrated. With this in mind, we then focused on how the Lagrangian geometry and kinematics determines the effective number of fields and how this number is reflected in the power spectra, bispectrum, and trispectrum. We pointed out that the effective number of fields needed to describe the background and perturbed solutions do not necessarily coincide, and we gave a simple method to determine the effective dimension of a multi-field system in the slow-roll limit. Next, we presented known formulas for the power spectra, discussed how the simplifications presented in this paper can greatly ease the calculation of the spectra, and then generalized the two-field expressions for the local non-Gaussianity parameters to multi-field inflation. We extended our two-field consistency relation [69] relating several of the cosmic observables to multi-field inflation, and we discovered a *multi-field observable* involving the cross spectrum that can potentially distinguish two-field models from models with three or more effective fields. However, being able to use the cross spectrum for this purpose requires knowledge of the post-inflationary history of the entropy modes. In the future, a better understanding of this post-inflationary evolution is essential in order to gain better insights into the spectral observables involving the isocurvature modes.

Stepping back and looking at the big picture, since more sensitive measurements of the spectral observables plus new spectral observables will reveal further clues into the nature of inflation, we must be posed to extract phenomenological information from these measurements. However, it is impractical to test the myriad inflationary models one by one against these measurements. Instead, we advocate studying classes of geometric and kinematical behaviors that arise from inflationary Lagrangians and determining how these behaviors affect the cosmic observables. This understanding can then be reversed and used to determine how constraints on spectral observables in turn constrain inflationary models, so that we can eventually put constraints on the inflationary Lagrangian that described our early Universe. The work presented in this paper represents a key step forward towards this ultimate goal.

VI. ACKNOWLEDGMENTS

This work was supported by an NSF Graduate Research Fellowship, NSF grants AST-0708534 and AST-

0908848, and a fellowship from the David and Lucile

Packard Foundation.

-
- [1] A. H. Guth, *Phys. Rev. D*, **23**, 347 (1981).
 - [2] A. D. Linde, *Particle Physics and Inflationary Cosmology* (Harwood: Switzerland, 1990).
 - [3] D. H. Lyth and A. Riotto, *Phys. Rep.*, **314**, 1 (1999).
 - [4] A. R. Liddle and D. H. Lyth, *Cosmological Inflation and Large-Scale Structure* (Cambridge Univ. Press: Cambridge, 2000).
 - [5] B. A. Bassett, S. Tsujikawa, and D. Wands, *Rev. Mod. Phys.*, **78**, 537 (2006).
 - [6] V. F. Mukhanov and G. V. Chibisov, *JETP Lett.*, **33**, 532 (1981).
 - [7] V. F. Mukhanov and G. V. Chibisov, *Sov. Phys. JETP*, **56**, 258 (1982).
 - [8] S. W. Hawking, *Phys. Lett. B*, **115**, 295 (1982).
 - [9] A. A. Starobinsky, *Phys. Lett. B*, **117**, 175 (1982).
 - [10] A. H. Guth and S.-Y. Pi, *Phys. Rev. Lett.*, **49**, 1110 (1982).
 - [11] J. M. Bardeen, P. J. Steinhardt, and M. S. Turner, *Phys. Rev. D*, **28**, 679 (1983).
 - [12] E. Komatsu *et al.*, *Astrophys. J. Suppl.* **192**, 18 (2011).
 - [13] C. M. Peterson and M. Tegmark, *Phys. Rev. D* **83**, 023522 (2011).
 - [14] H. Kodama and M. Sasaki, *Prog. Theor. Phys. Suppl.*, **78**, 1 (1984).
 - [15] D. S. Salopek, J. R. Bond, and J. M. Bardeen, *Phys. Rev. D*, **40**, 1753 (1989).
 - [16] D. S. Salopek, *Phys. Rev. D*, **52**, 5563 (1995).
 - [17] M. Sasaki and E. D. Stewart, *Prog. Theor. Phys.*, **95**, 71 (1996).
 - [18] T. T. Nakamura and E. D. Stewart, *Phys. Lett. B*, **381**, 413 (1996).
 - [19] M. Sasaki and T. Tanaka, *Prog. Theor. Phys.*, **99**, 763 (1998).
 - [20] J.-C. Hwang and H. Noh, *Phys. Lett. B*, **495**, 277 (2000).
 - [21] S. Groot Nibbelink and B. J. W. van Tent, arXiv:hep-ph/0011325 (2000).
 - [22] J.-C. Hwang and H. Noh, *Class. Quant. Grav.*, **19**, 527 (2002).
 - [23] S. Groot Nibbelink and B. J. W. van Tent, *Class. Quant. Grav.*, **19**, 613 (2002).
 - [24] J.-O. Gong and E. D. Stewart, *Phys. Lett. B*, **538**, 213 (2002).
 - [25] B. van Tent, *Class. Quant. Grav.*, **21**, 349 (2004).
 - [26] G. I. Rigopoulos, E. P. S. Shellard, and B. J. W. van Tent, *Phys. Rev. D*, **73**, 083521 (2006).
 - [27] H.-C. Lee, M. Sasaki, E. D. Stewart, T. Tanaka, and S. Yokoyama, *J. Cosmol. Astropart. Phys.* 10 (2005) 004.
 - [28] D. Langlois and S. Renaux-Petel, *J. Cosmol. Astropart. Phys.* 04 (2008) 017.
 - [29] V. F. Mukhanov and P. J. Steinhardt, *Phys. Lett. B*, **422**, 52 (1998).
 - [30] C. Gordon, D. Wands, B. A. Bassett, and R. Maartens, *Phys. Rev. D*, **63**, 023506 (2001).
 - [31] N. Bartolo, S. Matarrese, and A. Riotto, *Phys. Rev. D*, **64**, 083514 (2001).
 - [32] N. Bartolo, S. Matarrese, and A. Riotto, *Phys. Rev. D*, **64**, 123504 (2001).
 - [33] D. Wands, N. Bartolo, S. Matarrese, and A. Riotto, *Phys. Rev. D*, **66**, 043520 (2002).
 - [34] F. Di Marco, F. Finelli, and R. Brandenberger, *Phys. Rev. D*, **67**, 063512 (2003).
 - [35] F. Di Marco and F. Finelli, *Phys. Rev. D*, **71**, 123502 (2005).
 - [36] C. T. Byrnes and D. Wands, *Phys. Rev. D*, **74**, 043529 (2006).
 - [37] D. Langlois and F. Vernizzi, *J. Cosmol. Astropart. Phys.* 02 (2007) 017.
 - [38] Z. Lalak, D. Langlois, S. Pokorski, and K. Turzynski, *J. Cosmol. Astropart. Phys.* 07 (2007) 014.
 - [39] S. Renaux-Petel and G. Tasinato, *J. Cosmol. Astropart. Phys.* 01 (2009) 012.
 - [40] X. Gao, *J. Cosmol. Astropart. Phys.*, 02 (2010) 019.
 - [41] G. I. Rigopoulos, E. P. S. Shellard, B. J. W. van Tent, *Phys. Rev. D*, **72**, 083507 (2005).
 - [42] G. I. Rigopoulos, E. P. S. Shellard, and B. J. W. van Tent, *Phys. Rev. D* **73**, 083522 (2006).
 - [43] G. I. Rigopoulos, E. P. S. Shellard, and B. J. W. van Tent, *Phys. Rev. D* **76**, 083512 (2007).
 - [44] S. A. Kim and A. R. Liddle, *Phys. Rev. D* **74**, 063522 (2006).
 - [45] T. Battefeld and R. Easther, *J. Cosmol. Astropart. Phys.* 03 (2007) 020.
 - [46] D. Battefeld and T. Battefeld, *J. Cosmol. Astropart. Phys.* 05 (2007) 012.
 - [47] S. Yokoyama, T. Suyama, and T. Tanaka, *J. Cosmol. Astropart. Phys.* 07 (2007) 013.
 - [48] S. Yokoyama, T. Suyama, and T. Tanaka, *Phys. Rev. D* **77**, 083511 (2008).
 - [49] A. Misra and P. Shukla, *Nucl. Phys. B* **810**, 174 (2009).
 - [50] Q.-G. Huang, *J. Cosmol. Astropart. Phys.* 06 (2009) 035.
 - [51] C. T. Byrnes and K.-Y. Choi, *Adv. Astron.* **2010**, 724525 (2010).
 - [52] T. Tanaka, T. Suyama, and S. Yokoyama, *Class. Quant. Grav.* **27**, 124003 (2010).
 - [53] S. A. Kim, A. R. Liddle, and D. Seery, *Phys. Rev. Lett.* **105**, 181302 (2010).
 - [54] N. Bartolo, S. Matarrese, and A. Riotto, *Phys. Rev. D* **65**, 103505 (2002).
 - [55] F. Bernardeau and J.-P. Uzan, *Phys. Rev. D* **66**, 103506 (2002).
 - [56] F. Bernardeau and J.-P. Uzan, *Phys. Rev. D* **67**, 121301 (2003).
 - [57] F. Vernizzi and D. Wands, *J. Cosmol. Astropart. Phys.* 05 (2006) 019.
 - [58] K.-Y. Choi, L. M. H. Hall, and C. van de Bruck, *J. Cosmol. Astropart. Phys.* 02 (2007) 029.
 - [59] C. T. Byrnes, K.-Y. Choi, and L. M. H. Hall, *J. Cosmol. Astropart. Phys.* 10 (2008) 008.
 - [60] A. C. Vincent and J. M. Cline, *J. High Energy Phys.* 10 (2008) 093.
 - [61] T. Wang, *Phys. Rev. D* **82**, 123515 (2010).
 - [62] J. Meyers and N. Sivanandam, *Phys. Rev. D*, **83**, 103517 (2011).
 - [63] M. Sasaki, *Prog. Theor. Phys.*, **76**, 1036 (1986).
 - [64] V. F. Mukhanov, *Soviet Phys. JETP*, **68**, 1297 (1988).

- [65] A. Taruya and Y. Nambu, *Phys. Lett. B*, **428**, 37 (1998).
- [66] L. Amendola, C. Gordon, D. Wands, and M. Sasaki, *Phys. Rev. Lett.*, **88**, 211302 (2002).
- [67] A. A. Starobinskii, *JETP Lett.*, **30**, 683 (1979).
- [68] S. Blanes, F. Casas, J. A. Oteo, and J. Ros, *Phys. Rep.* **470**, 151 (2009).
- [69] C. M. Peterson and M. Tegmark, *Phys. Rev. D*, **84**, 023520 (2011).
- [70] P. Creminelli and M. Zaldarriaga, *J. Cosmol. Astropart. Phys.* 10 (2004) 006.
- [71] D. H. Lyth and Y. Rodriguez, *Phys. Rev. Lett.* **95**, 121302 (2005).
- [72] L. Alabidi and D. Lyth, *J. Cosmol. Astropart. Phys.* 05 (2006) 016.
- [73] C. T. Byrnes, M. Sasaki, and D. Wands, *Phys. Rev. D* **74**, 123519 (2006).
- [74] T. Suyama and M. Yamaguchi, *Phys. Rev. D* **77**, 023505 (2008).